









## Removal of metals from water using MOF-based composite adsorbents

Cite this: *Environ. Sci.: Water Res. Technol.*, 2023, 9, 1305

Farnaz Zadehahmadi, <sup>\*a</sup> Nathan T. Eden, <sup>a</sup> Hamidreza Mahdavi, <sup>a</sup>  
Kristina Konstas,<sup>b</sup> James I. Mardel,<sup>b</sup> Mahdokht Shaibani, <sup>c</sup>  
Parama Chakraborty Banerjee <sup>a</sup> and Matthew R. Hill <sup>\*ab</sup>

Received 12th December 2022,  
Accepted 2nd March 2023

DOI: 10.1039/d2ew00941b

rsc.li/es-water

Metal-organic frameworks (MOFs)-based composites have attracted significant research interest, especially in the removal of metal ion pollutants from water. MOFs are regarded as excellent metal ion adsorbents due to their large surface area, tuneable pores, and abundance of active sites. MOF composites, in which MOFs are combined with a variety of materials such as magnetic particles, various polymers, and graphene oxide, have been developed to enhance the metal adsorption capacity of MOFs. This article provides an overview of the current MOF-based composites used as superior sorbents. In addition, their synthesis techniques, applications, and performance are discussed and compared with those of pure MOFs and other adsorbents.

### Water impact

Metals in water can negatively impact human and environmental health and will be future mining priorities. Adsorption separation by MOF composites is a new field that simultaneously enhances adsorption efficacy, facilitates physical handling, and reduces secondary pollution. In this review paper, we reveal significant trends in which MOF composites outperform conventional adsorbents, including reagent-free, sustainable regeneration.

## Introduction

The provision of safe drinking water is an essential prerequisite for a healthy lifestyle. A key challenge for public health is the removal of metal ions from the water supply system. Metal ions enter the water supply system in various ways; natural or anthropogenic sources such as dissolution from water pipes, mining, fertilizers, and radioactive waste from nuclear power stations.<sup>1</sup> Anthropogenic release of metals into the environment is possible through three potential pathways – air, solid and liquid routes. In the air, released flues and particulates from mining and industry can be directly settled into water bodies or travel with the water cycle.<sup>2</sup> Improper disposal of metal waste products into the ocean or waterways initiates metal ion leaching. Liquid wastes generated from mining, refining, industrial processes, and landfills travel through the environment until reaching the ocean or other waterways.<sup>3</sup>

The World Health Organization (WHO) published the maximum contaminant level (MCL) of a variety of contaminants including metal ions in drinking water. As well as being necessary for environmental and public health purposes, the adsorption of metal ions waste is also economically beneficial.<sup>4,5</sup>

Methods explored to date for metal removal from water include chemical precipitation, ion exchange, membrane filtration, electrochemical treatment technologies, and adsorption; the latter is the most effective technology used for water remediation.<sup>6–9</sup>

Metal oxides, porous carbon materials, bio-adsorbents, and zeolites are commonly used for the adsorption of metals from water.<sup>10–16</sup> Metal-organic frameworks (MOFs) are a class of porous adsorbent materials that have been investigated for various applications over the past three decades.<sup>17–19</sup> Due to their tuneability and high surface area, metal-organic frameworks have been used widely either in their pristine or post-functionalised forms. Functionalized forms include the hybridization or coating of pristine MOFs with various functional groups like amines, sulfates, hydroxides, and alkyl chains.

Presented in Fig. 1 is a brief schematic history of MOFs and their applications in the removal of metal ions from water. In 1989, the first deliberately designed infinite polymeric framework,  $(\text{Cu}^{\text{I}}[\text{C}(\text{C}_6\text{H}_4\text{CN})_4])_n^{n+}$  was synthesised

<sup>a</sup> Department of Chemical and Biological Engineering, Monash University, Australia. E-mail: Farnaz.Zadehahmadi@monash.edu, Matthew.Hill@monash.edu

<sup>b</sup> CSIRO Manufacturing, Bag 10, Clayton South, VIC 3169, Australia. E-mail: Matthew.Hill@csiro.au

<sup>c</sup> Department of Chemical and Environmental Engineering, RMIT University, Australia



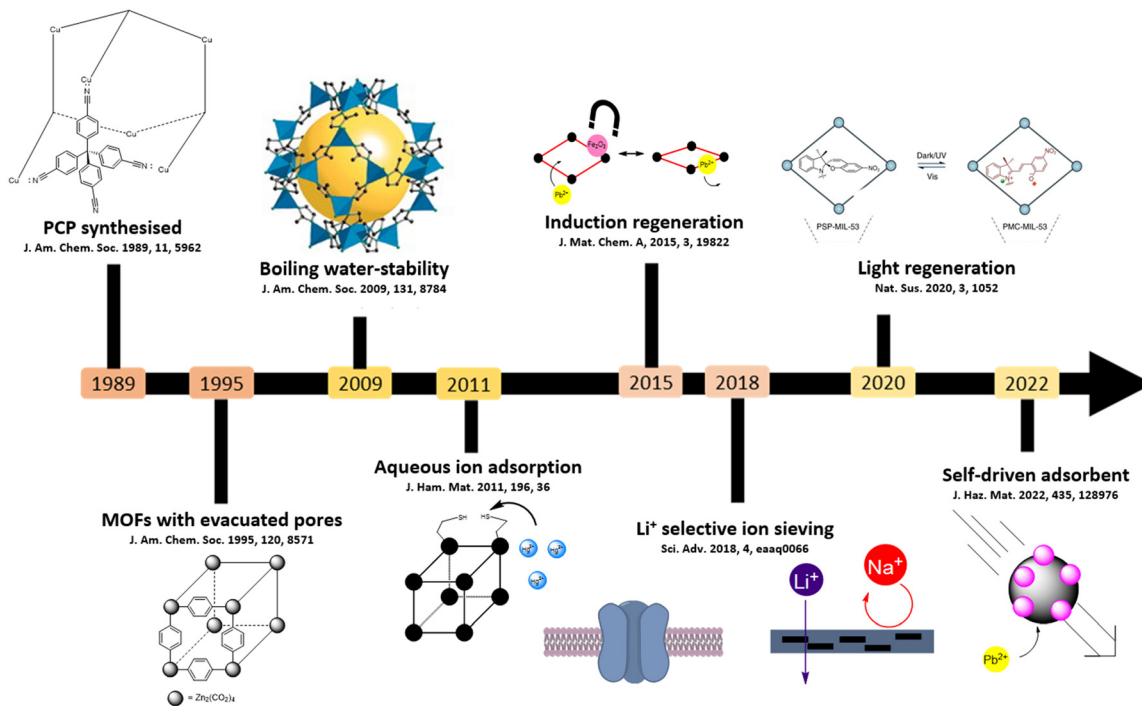


Fig. 1 Timeline of relative achievements for the removal of metals from water using MOFs, both by batch and continuous mechanisms.

and its structure was determined by single X-ray crystallography. By 1998, the development and understanding of the chemistry and porosity of MOFs were established. An early example was  $Zn_3(bdc)_3 \cdot 6CH_3OH$ , demonstrating the importance of guest molecule removal using a series of solvent exchanges to expose the internal metal sites and porosity within the framework.<sup>20,21</sup> Water-stability was first recognised in 2009 when a sodalite-type MOF  $H_3[(Cu_4Cl)_3(BTTr)_8(DMF)_{12}] \cdot 7DMF \cdot 76H_2O$  was prepared and by 2015, MOFs were being explored for aqueous ion-capture with the adsorption of  $Cu^{II}$  in water by MOF-5.<sup>22,23</sup> ZIF-8, the first MOF with  $>1000 \text{ mg g}^{-1}$  adsorption capacity, was reported in 2018 to adsorb  $Pb^{II}$  in aqueous solution, and a nanoscale ZIF-8 membrane was developed to separate alkali metals.<sup>24,25</sup> Earlier in 2019, a  $UiO-66-NH_2$  nanoscale membrane was observed to have a selectivity of  $Li^I$  to  $Mg^{II}$  of around 20, the highest ever reported selectivity for these cations.<sup>26</sup> Materials that adsorb in batch and flow are quite different, and in this perspective, we focus on batch adsorption materials.

As it is shown in Table 1, many pristine MOF materials have been found to adsorb metals from water. In some cases, these MOFs have shown remarkable adsorption kinetics and capacities ( $>1 \text{ g ion per g MOF}$ ).<sup>27</sup> While MOFs were originally developed to adsorb heavy metals, such as As, Pb, Hg, or Cr, the increase in lithium demand has led to a new focus on lithium separation.<sup>28,29</sup> MOFs have shown promising properties for use in metal removal by adsorption mechanism (Table 1). The ultrahigh surface area of this class of materials plays the key role in the large uptake capacity of the metals. A careful engineering of the pores promotes the capacity of the MOFs by incorporating

functional groups that may contribute to their enhanced affinity for metal ions.

It is worth noting that several groups have utilized thiol groups, which enhance affinity towards heavy metal ions by interacting preferentially between soft acids and soft bases. A further benefit of this approach is that it helps to increase the selectivity towards the heavy metal ions even when the common essential metal ions present in the drinking water are also present. It has also been found that adding additional free hydroxyl or carboxylic groups to the linkers enhances the adsorption capacities by means of coordination and electrostatic interactions. Furthermore, some anionic MOFs have been found to be capable of capturing and removing heavy metal ions by substituting the counterions with the heavy metal ions.

There have been numerous reviews pertaining to the removal of metals by pristine MOF materials and functionalized MOFs in the literature as it is summarized in Table 1.<sup>9,30–32</sup> Besides the pure MOFs and functionalized MOFs, less attention has been paid to categorizing MOF-composites separately and studying the effects of adding other materials to pure MOFs on metal removal from water.

In general, the use of hybrid materials is motivated by three factors: improved stability, easy handling, and reusability.

Thus, in this review paper, we have discussed various MOF-composites and the effect of combining MOFs with other materials, such as polymers, carbon-based materials, and magnetic particles to enhance their ability to remove metals from water. Here, our discussion focuses only on the removal of metals from water, rather than other



**Table 1** Overview of pure MOFs as adsorbents for metals in aqueous systems. This table is organised by metals, the MOF adsorbents by their maximum uptake and also the charge on the metal, the concentration of metal chloride to cause health effects,<sup>5</sup> that are listed, and sources of the metal to enter the water<sup>37</sup>

| Metal/metalloid          | The concentration of MCL causes health effects (mg L <sup>-1</sup> ) | MOF adsorbent   | Maximum MOF capacity (mg g <sup>-1</sup> ) | Source of metal in water   | Potential Health effects from long-term exposure above the MCL (unless specified as short-term)                                       | Ref.         |
|--------------------------|--|---|--|--|---|--------------|
| Antimony(v)              | 0.006  | NU-1000   | 287.88                                     | Discharged ammunition  | An increase in blood cholesterol, and a decrease in blood sugar, may cause direct lung damage and carcinogenesis                      | 38           |
| Antimony(III)            |  | NU-1000   | 136.97                                     |  |   | 38           |
| Arsenic(v)               | 0.01   | Zn-MOF-74   | 325  | Metal manufacturing, wood treatments, glasses, petroleum and coal-derived chemicals, combustion of fossil fuels  | Skin manifestations, visceral cancers, vascular disease, carcinogenesis in bladder, lung, skin, neurotoxicity, diabetes               | 39           |
|                          |  | UiO-66  | 303.4                                      |  |   | 40           |
|                          |  | AUBM-1  | 103.1                                      |  |   | 41           |
|                          |  | MIL-100(Fe)   | 110  |  |   | 42           |
|                          |  | H-ZIF-8-14  | 90.92                                      |  |   | 43           |
|                          |  | ZIF-8   | 76.5                                       |  |   | 43           |
|                          |  | H-ZIF-8-12  | 74.08                                      |  |   | 43           |
|                          |  | H-ZIF-8-11  | 72.67                                      |  |   | 43           |
|                          |  | ZIF-8-MeOH  | 72.33                                      |  |   | 43           |
|                          |  | Arsenic(III)  |  |  |   | Fe-Co-MOF-74 |
| Zn-MOF-74                | 211  |   |  | 39   |   |              |
| UiO-66                   | 202  |   |  | 40   |   |              |
| UiO-66-(SH) <sub>2</sub> | 40   |   |  | 45   |   |              |
| Barium(II)               | 2  | Zr-bdc-NH <sub>2</sub> -SO <sub>4</sub>               | 181.8                                      | Typically insoluble, mining, leaching from hazardous waste sites   | Increase in blood pressure, cardiac arrhythmia, paralysis, decrease in weight, kidney damage  | 46           |
|                          |  | MOF-808-SO <sub>4</sub>                               | 131.1                                      |  |   | 47           |
|                          |  | MIL-101-Cr-SO <sub>3</sub> H                          | 70.5                                       |  |   | 47           |
| Cadmium(II)              | 0.005  | MOF-808-EDTA  | 528  | Metal treatments, combustion of coal and oil, tobacco, volcanic emission, tire wearing, electronics  | Kidney tubular damage, respiratory irritation, osteoporosis, osteomalacia, renal tubular damage, carcinogenesis                       | 48           |
|                          |  | FJI-H9  | 225  |  |   | 49           |
|                          |  | NH <sub>2</sub> -Zr-MOF                               | 177.35                                     |  |   | 50           |
|                          |  | Cu <sub>3</sub> (BTC) <sub>2</sub> -SO <sub>3</sub> H | 88.7                                       |  |   | 51           |
|                          |  | UiO-66-NHC(S)NHMe                                     | 49   |  |   | 52           |
|                          |  | TMU-4   | 48   |  |   | 53           |
|                          |  | TMU-5   | 43   |  |   | 53           |
|                          |  | TMU-6   | 41   |  |   | 53           |
| Chromium(vi)             | 0.1  | 1D Fe-gallic acid                                     | 1709.2                                     | Chemical manufacturing, incinerators, combustion of coal and oil, volcanic emission, leather tanning, electrical manufacturing, textiles, radioactive wastes | Allergic dermatitis, carcinogenesis for Cr(vi), gastrointestinal ulcers, renal damage, central nervous system damage for Cr(III)      | 54           |
|                          |  | ZJU-101   | 245  |  |   | 55           |
|                          |  | SCNU-Z1-Cl  | 241  |  |   | 56           |
|                          |  | FIR-54  | 103  |  |   | 57           |
|                          |  | Zn-Co-SLUG-35   | 68.5                                       |  |   | 58           |
|                          |  | 1-ClO <sub>4</sub>                                    | 63   |  |   | 59           |
|                          |  | SLUG-21   | 62.88                                      |  |   | 60           |
|                          |  | Cu-BTC  | 48   |  |   | 61           |
|                          |  | 1-NO <sub>3</sub>                                     | 37   |  |   | 62           |
|                          |  | Chromium(III)   |  |  |   | TMU-4        |
| TMU-5                    | 123  |   |  | 53   |   |              |
| TMU-6                    | 118  |   |  | 53   |   |              |
| Cobalt(II)               | 0.04   | UiO-66-Schiff   | 256  | Steel-related manufacturing, paints and varnish leaching, inks, volcanic emissions   | Skin irritation (short-term exposure), mammalian DNA damage, reproductive effects, sensitisation of skin, polycythemia, heart failure | 63           |
|                          |  | MOF-808-EDTA  | 150  |  |   | 48           |
|                          |  | TMU-5   | 63   |  |   | 53           |
|                          |  | TMU-6   | 59   |  |   | 53           |
|                          |  | TMU-4   | 55   |  |   | 53           |
| Copper(II)               | 1.3  | ZIF-67  | 617.51                                     | Biological complexes, mining and manufacture of copper metals, chemical manufacturing, concrete and related products, marine antifouling paint               | Gastrointestinal distress, nausea, anaemia, seizures (short-term exposure), liver or kidney damage and failure                        | 25           |
|                          |  | ZIF-8   | 454.72                                     |  |   | 25           |
|                          |  | MOF-808-EDTA  | 155  |  |   | 48           |
|                          |  | TMU-4   | 62   |  |   | 53           |
|                          |  | TMU-6   | 60   |  |   | 53           |
|                          |  | TMU-5   | 57   |  |   | 53           |



Table 1 (continued)

| Metal/metalloid         | The concentration of MCL causes health effects (mg L <sup>-1</sup> ) | MOF adsorbent  | Maximum MOF capacity (mg g <sup>-1</sup> ) | Source of metal in water   | Potential Health effects from long-term exposure above the MCL (unless specified as short-term)  | Ref. |
|-------------------------|--|--|--|--|--|------|
| Iron(III)               | ~200   | MOF-808-EDTA   | 150  | Pigments, manufacturing, rusting   | Vomiting, tachycardia, vision loss, cardiopulmonary arrest (short-term effect), haemorrhagic necrosis  | 48   |
| Lead(II)                | 0.015  | ZIF-67   | 1348.42                                    | Mining and manufacturing, coal mining, concrete and related production, leaching from landfill, batteries                              | Competitive binding with many cations in proteins and receptors (short-term), delay in physical or mental development, slight deficits in attention span and learning abilities (for infants and children), kidney problems or high blood pressure | 25   |
|                         |  | ZIF-8  | 1190.80                                    |  |  | 25   |
|                         |  | MOF-808-EDTA   | 313  |  |  | 48   |
|                         |  | TMU-5  | 251  |  |  | 53   |
|                         |  | TMU-4  | 237  |  |  | 53   |
|                         |  | UiO-66-NHC(S)NHMe  | 232  |  |  | 52   |
|                         |  | TMU-6  | 224  |  |  | 53   |
|                         |  | NH <sub>2</sub> -Zr-MOF  | 92.18                                      |  |  | 50   |
| MIL-101(Cr)             | 15.78  | 64   |  |  |  |      |
| Lithium(I)              | 20   | Zn-MOF5-12c4   | 12.3                                       | Batteries, leaching from landfill  | Nervous system damage, sensory system damage, neurological damage  | 65   |
|                         |  | LMOF-321   | 12.18                                      |  |  | 29   |
|                         |  | MIL-121-a  | 3.89                                       |  |  | 28   |
| Magnesium(II)           | 8100   | MIL-121-a  | 6.08                                       | High-temperature industry usages   | Reported number for LD50-oral rats, impaired neuromuscular transmission  | 28   |
|                         |  | MOF-808-EDTA   | 63   |  |  | 48   |
| Manganese(VII)          | 0.05   | SCNU-21  | 292  | Ore processing, landfill leaching  | Neurotoxicity, congestion of blood vessels, ocular damage and necrosis in rabbit testing, mobility and motor control reduction in monkeys  | 56   |
| Mercury(II) (inorganic) | 0.002  | CaCu <sub>6</sub> [(S,S)-methox] <sub>3</sub> (OH) <sub>2</sub> (H <sub>2</sub> O) | 900  | Weathering, volcanic activity, leaching from gold mining, coal burning, copper/lead manufacturing, battery leaching                    | Mania, sensitivity, neurological damage, renal failure, circulatory collapse, (short-term exposure), biomagnification in aquatic environments, limited evidence for carcinogenicity, inhibition of amino acid transport, spontaneous abortions     | 66   |
|                         |  | JUC-62   | 836.7                                      |  |  | 67   |
|                         |  | UiO-66-NHC(S)NHMe  | 769  |  |  | 52   |
|                         |  | MOF-808-EDTA   | 592  |  |  | 48   |
|                         |  | FJI-H12  | 439.8                                      |  |  | 68   |
|                         |  | LMOF-263   | 380  |  |  | 69   |
|                         |  | PCN-100  | 364.7                                      |  |  | 70   |
|                         |  | UiO-66-(SH) <sub>2</sub>   | 236.4                                      |  |  | 71   |
|                         |  | MIL-101-NH <sub>2</sub>  | 30.67                                      |  |  | 72   |
|                         |  | ZIF-90-SH  | 22.45                                      |  |  | 73   |
| Nickel(II)              | 0.1  | MOF-808-EDTA   | 155  | Fossil fuel combustion, waste incineration, wastewater from sewage treatment, stormwater runoff, landfill leaching, volcanic emissions | Contact dermatitis, asthma, chronic respiratory infections   | 48   |
| Selenium(VI)            | 0.05   | NU-1000  | 62   | Combustion of coal and oil, metal smelting and refining, incinerators, electronic photographic waste leaching, weathering              | Hair or fingernail loss, numbness in fingers or toes or circulation problems, kidney failure, heart failure  | 74   |
|                         |  | UiO-66-(NH) <sub>2</sub>   | 38.5                                       |  |  | 75   |
|                         |  | UiO-66-HCl   | 86.8                                       |  |  | 76   |
| Selenium(IV)            |  | NU-1000  | 102  | Photographic waste, sewage, metal production, urban runoff, soil erosion, textile effluent   | Fatty degeneration of the liver, kidneys, agyria   | 74   |
|                         |  | UiO-66-(NH) <sub>2</sub>   | 45   |  |  | 75   |
| Silver(I)               | 0.000001   | MIL-53(Al)   | 183  |  |  | 77   |



Table 1 (continued)

| Metal/metalloid | The concentration of MCL causes health effects (mg L <sup>-1</sup> ) | MOF adsorbent              | Maximum MOF capacity (mg g <sup>-1</sup> ) | Source of metal in water   | Potential Health effects from long-term exposure above the MCL (unless specified as short-term)                | Ref. |
|-----------------|--|----------------------------|--|--|--|------|
| Thallium(IV)    | 0.002  | UiO-66-(COOH) <sub>2</sub> | 350  | Cement manufacture, coal power plants, volcanic activity   | Hair loss, blood change, problems with kidneys, intestines or liver  | 78   |
|                 |  | dMn-MOF                    | 46.35                                      |  |  | 79   |
| Uranium(VI)     | 0.000002   | HKUST-1                    | 787.4                                      | Mining of uranium, leaching from depleted uranium  | UCl <sub>4</sub> hydrolyses to insoluble UCl <sub>2</sub> in the body. Lung damage, kidney damage, weight loss | 80   |
|                 |  | MIL-101-DETA               | 350  |  |  | 81   |
|                 |  | MOF-76                     | 298  |  |  | 82   |
|                 |  | MOF-2                      | 217  |  |  | 83   |
| Zinc(II)        | 73   | MOF-3                      | 109  | Zinc manufacturing and mining, sewage treatment, corrosion of galvanised material, fertilisers, battery waste leaching | Relatively not detrimental to mammals (may affect cholesterol metabolism in humans)                            | 83   |
|                 |  | MOF-808-EDTA               | 161  |  |  | 48   |

contaminants such as dyes or organic pollutants, which are discussed in detail in other review articles.<sup>33–35</sup>

## Water-stable MOFs

In order to be effective at removing metal ions from water, the MOF must remain stable after multiple cycles of metal capture and regeneration. Our discussion will therefore focus on water-stable MOF-based composites and the methods used to make the MOFs water-stable in order to be suitable for the removal of metal ions from water.

Several methods have been used to evaluate the stability of MOFs in water, often by comparison of the pre- and post-exposed material characteristic data. A comparison of the powder X-ray diffraction (PXRD) patterns can establish whether any small-scale structural changes have occurred. Measuring the surface area and porosity of the exposed MOF is essential as it can indicate the collapse of the MOF pores. The functional groups of linkers and coordination environment around the structural building units (SBUs) should also remain present, this can be monitored by infrared spectroscopy or X-ray Photoelectron Spectroscopy (XPS). The total removal of water from the pores and thermal stability can be determined by thermogravimetric analysis (TGA). Using electron microscopy, defects can be observed in the nm to micron range. For complete monitoring and understanding of the effects of water exposure to MOFs, a variety of techniques that analyse multiple time and length scales may be used to establish MOF stability in water and the operating conditions.<sup>36</sup>

Judicious choice of metals and linkers allows tuning of the stability of MOFs with desirable properties, such as the use of hard and soft donor atoms, the number of these

bonds, hydrophobicity/philicity, steric blocking around the node SBU and introduction of additives (Fig. 2).

Utilising the Pearson hard-soft acid-base (HSAB) theory, hard acid-base MOFs, such as the UiO series, and soft acid-base MOFs, such as zeolitic imidazolate frameworks (ZIFs) have extensively been synthesised and shown to be water stable. Functional groups on linkers impart the MOF with many desirable properties, bulky nonpolar groups in particular impart increased hydrophobicity. Steric blocking of the metal node prevents access of water to the metal-linker bonds, preventing hydrolysis.<sup>84–87</sup>

Fluorination or the addition of long alkyl side chains to MOF ligands also reduces water intake. In a direct comparison, hydrophilic UiO-66-NH<sub>2</sub>, formed of Zr<sub>6</sub>O<sub>8</sub> clusters and 2-amino-1,4-benzenedicarboxylate, was post-synthetically modified with isostearyl chloride to give hydrophobic UiO-66-NHCOR (Fig. 3a).<sup>88</sup> This chemical treatment increased UiO-66-NHCOR contact angle of water on the surface from 32° to 158°. A fluorination example can

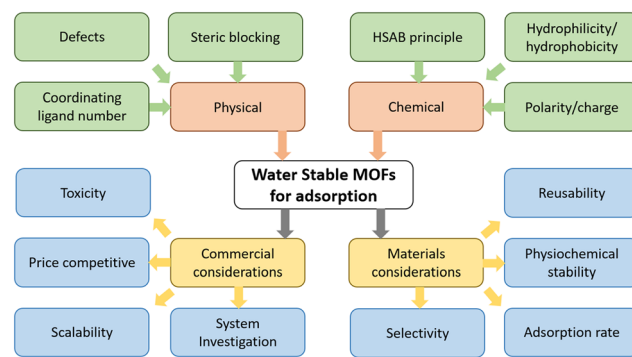
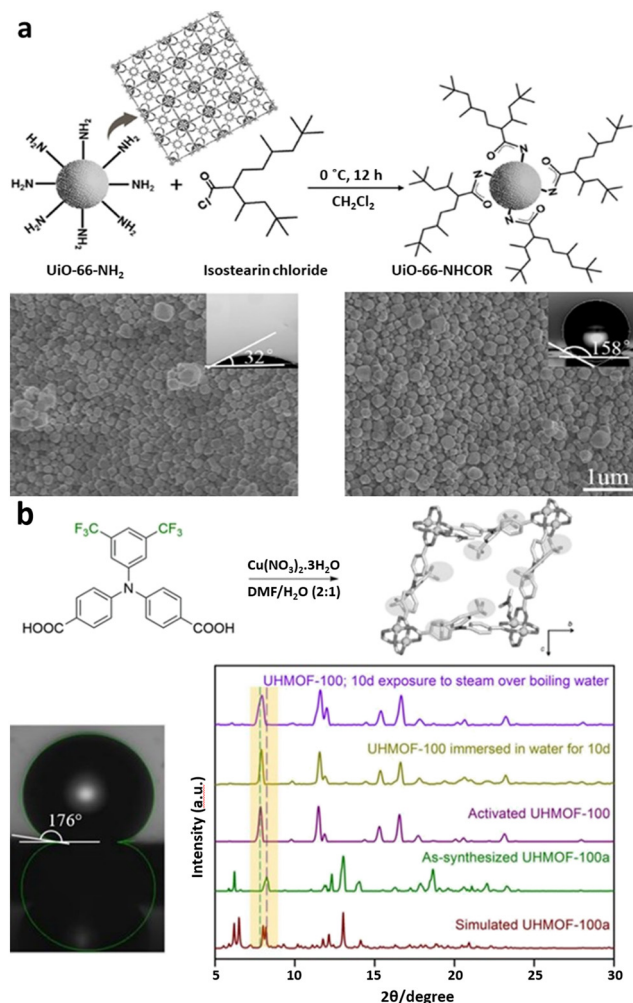


Fig. 2 Conceptual map for the design of water-stable MOFs for adsorption of metals from water.





**Fig. 3** (a) Post-synthetic modification of UiO-66-NH<sub>2</sub> with isostearin chloride to reduce hydrophilicity (reproduced from ref. 88 with permission from Elsevier Inc., copyright 2019). (b) Synthesis of UHMOF-100, with the use of trifluoromethyl groups on the ligand to generate an ultra hydrophobic MOF (reproduced from ref. 89 with permission from Wiley, copyright 2016).

be seen in the direct synthesis of UHMOF-100, composed of Cu paddlewheels and the fluorinated 4,4'([3,5-bis(trifluoromethyl)phenyl]azanediyldibenzoate) ligand, that demonstrated a water contact angle of 176°, the highest recorded in the literature (Fig. 3b).<sup>89</sup>

Comparison of vacated and water-infused UHMOF-100 PXRD patterns demonstrated that the initial MOF structure was retained. Such modification or designed synthesis may impart hydrophobicity to a MOF, but may also reduce its other desirable properties, such as surface area for metal adsorption or blocking of pore windows with bulky side chains. Therefore, other methods of imparting stability have also been investigated. An archetypical carboxylate MOF is UiO-66, with a 12-connected Zr<sub>6</sub>O<sub>4</sub>(OH)<sub>4</sub> SBU cluster formed from coordination to 1,4-benzenedicarboxylate ligands.<sup>90,91</sup> The Zr<sub>6</sub> node within the UiO-66 family of MOFs exhibits stability towards chemical stresses. This is a result of the

high oxidation state of the zirconium(IV) and the negatively charged carboxylate linkers that provide strong electrostatic forces of attraction, known as Coulombic interactions.<sup>92</sup> UiO-66 is found to be stable in saline water solutions for up to 100 days at 50 °C.<sup>93</sup> In addition, UiO-66 was able to maintain its crystallinity structure under acidic and basic pH treatments using PXRD for verification but the surface area was affected.<sup>91,92</sup>

Functional derivatives on the aromatic ring such as -NH<sub>2</sub>, -COOH, -SO<sub>3</sub>H or -CH<sub>3</sub> can be prepared and provide additional functionality and post-synthetic modification routes. A comprehensive hydrothermal and chemical stability study was investigated by Van Der Voort and co-authors. The study revealed the amine functionalised UiO-66, (UiO-66-NH<sub>2</sub>) retained crystallinity after exposure to peroxide, water or a pH = 12 solution over 3 days.<sup>92</sup> Other MOFs based on the Zr<sub>6</sub>O<sub>8</sub> cluster, BUT-12 and BUT-13, show little variation in crystallinity after treatment in boiling water for 24 h, and consistent porosity after treatment in boiling water for 7 d, 6 M HCl and NaOH solutions (pH = 10) for 24 h. The prevalence of high valence clusters including Zr<sub>6</sub>O<sub>8</sub> is key to achieving water stability in these MOFs.<sup>94</sup>

Similarly, soft acid–base coordination has been extensively observed in water-stable MOFs, most commonly in the zeolitic imidazolate framework (ZIF) family of MOFs, formed of soft metals such as Zn and derivatives of the imidazole organic linker.<sup>95,96</sup> ZIF-8, formed of 1-*H*-2-methylimidazole and Zn is stable in water, acidic and basic conditions, (pH: 4 to 12) for a period of 3 days at room temperature and 1 day in boiling 8 M NaOH solution.<sup>85,92</sup>

The role of the ligand towards MOF stability has been also been investigated. Construction of MOFs using a series of benzoate-derived tetracarboxylate ligands with increasing central rigidity demonstrated fixation of ligand rotation by steric blocking or by the inclusion of conjugated  $\pi$ -systems.<sup>97</sup> MOF UiO-67 is formed from 1,4-diphenyl dicarboxylate ligands, this system displays rotation around the biphenyl system and is susceptible to hydrolysis. When methyl groups are present on the biphenyl motif rotation was prohibited, and enhanced water stability was reported by Lillerud and co-authors.<sup>98</sup> Zhou and co-authors further investigated the rigidification of ligands by introducing pyrene motifs which exhibited stability against water and pH. Overall, the 13 Zr-MOFs developed by Zhou and co-workers showed a trend where more rigid hexamethyl and pyrene centred ligands, improved water stability, cyclability and chemical resistance.<sup>97</sup>

A general summary of factors to guide the synthesis of new MOFs for removal of metals from water include: 1. high charge MOF node ions or ion clusters to impart stability in water, 2. fluorination of the linker or other forms of hydrophobicity to increase stability, 3. green synthetic methods with cheaper materials to reduce environmental impact of preparation, 4. choice of functional group targeting selectivity towards the metal of interest, a. for ion exchange-type mechanisms, using an acidic functional group, b.



recyclability by acid or base regeneration, or ideally reagent-free regeneration, 5. hierarchically structured to improve diffusion properties, 6. further combination with other functional materials to prepare MOF composites.

## Metal uptake in MOF-based composites

MOFs are microporous materials with metal-containing nodes and interconnected organic linkers. MOFs can form extensive crystalline structures with molecular-dimension voids and channels accessible through pores.<sup>99</sup> In spite of this, the commercialization of MOFs has been limited by their crystalline or microcrystalline (*e.g.*, powder) form. There are several drawbacks to such powders, among them mass transfer restrictions, high-pressure drops, entrainment in packed beds, and handling difficulty due to dust formation,

which makes them difficult to incorporate into many technologies.<sup>100,101</sup> Thus, MOF-based composites with processable form factors are therefore being developed to increase their utility by combining their properties with those of other functional materials, such as polymers, aerogels, graphene oxide and magnetic materials.<sup>102–104</sup>

Thanks to MOFs' diverse properties such as highly porous nature, chemical diversity, structural tailorability, low costs, and large-scale production, as well as properties of their composites with other functional materials such as morphological, mechanical, physicochemical, and functional properties, there are numerous opportunities for preparing MOF composite materials with outstanding performance in a variety of fields.<sup>105,106</sup> Moreover, MOF-based composites are capable of improving the adsorption performance of MOFs when compared with MOFs on their own, due to the synergy between different components.<sup>102,107</sup>

**Table 2** Summary of the adsorptive capability of MOF-based composites in the removal of metals from water

| Composites                | Components  | Target metal                 | Adsorption capacity (mg g <sup>-1</sup> ) | Ref.   |
|---------------------------|---|------------------------------|---|--------|
| Polymer/MOF               | PDA/Fe–BTC  | Pb(II)/Hg(II)                | 394/1634                                  | 114    |
|                           | Fe–BTC/PDA MACPs  | Pb(II)/Pd                    | 230/496                                   | 116    |
|                           | PAN/ZIF-8   | U(VI)                        | 530                                       | 30     |
|                           | PPy/ZIF-8   | U(VI)                        | 534                                       | 115    |
|                           | PAN/MOF-808   | Cd(II)/Zn(II)                | 225/287                                   | 121    |
|                           | PAN/MOF-F300  | Hg(II)/Pb(II)                | 53/30                                     | 122    |
|                           | PAN/MOF-808   | Hg(II)/Pb(II)                | 51/24                                     | 122    |
|                           | PVDF/MOF-808  | Hg(II)/Pb(II)                | 43/17                                     | 122    |
|                           | Chitosan/MIL-125  | Pb(II)                       | 407                                       | 119    |
|                           | Chitosan/UiO-66–chitosan  | Cu(II)/Ni(II)/Cr(VI)         | 51/60/94                                  | 120    |
| Aerogels/MOF              | UiO-66-NH <sub>2</sub> @CA  | Pb(II)/Cu(II)                | 89/39                                     | 123    |
|                           | UiO-66@CA   | Pb(II)/Cu(II)                | 81/31                                     | 123    |
|                           | ZIF-8@CA  | Cr(IV)                       | 41.8                                      | 124    |
|                           | UiO-66@CNC  | Cr(VI)                       | 3.89                                      | 125    |
|                           | BC@ZIF-8  | Pb(II)/Cd(II)                | 390/220                                   | 126    |
|                           | Graphene oxide/MOF  | GO-MIL-101(Fe)               | U(VI)                                     | 106.89 |
| GO–COOH/UiO-66            |   | U(VI)                        | 1002                                      | 128    |
| Cu(tpa)·GO                |   | Pb(II)/Cu(II)/Zn(II)         | 88/243/131                                | 129    |
| Magnetic framework        | MP@ZIF-8  | Cr(VI)                       | 136.5                                     | 130    |
|                           | γ-Fe <sub>2</sub> O <sub>3</sub> /C@HKUST-1   | Cr(VI)                       | 101.4                                     | 131    |
|                           | MFC (magnetic framework composites)   | Pb(II)                       | 492                                       | 132    |
|                           | Magnetic MOF nanocomposite  | Cd(II)/Pb(II)/Ni(II)/Zn(II)  | 188/104/98/206                            | 133    |
|                           | (magnetic MOF-DHz nanocomposite)  |                              |   |        |
|                           | Fe <sub>3</sub> O <sub>4</sub> @AMCA-MIL53(Al)  | U(VI)/Th(IV)                 | 227.3/285.7                               | 134    |
|                           | Thiol-functionalized Fe <sub>3</sub> O <sub>4</sub> @Cu <sub>3</sub> (btc) <sub>2</sub> | Hg(II)/Pb(II)                | 348/215                                   | 135    |
|                           | Fe <sub>3</sub> O <sub>4</sub> @ZIF-8   | As(III)                      | 100                                       | 136    |
|                           | Fe <sub>3</sub> O <sub>4</sub> @SiO <sub>2</sub> @HKUST-1                               | Hg(II)                       | 264                                       | 137    |
|                           | MOF/Fe <sub>3</sub> O <sub>4</sub> /KNiFC   | Sr(II)                       | 90  | 138    |
|                           | Cu-MOFs/Fe <sub>3</sub> O <sub>4</sub>  | Pb(II)                       | 219                                       | 139    |
|                           | Fe <sub>3</sub> O <sub>4</sub> –ethylenediamine/MIL-101(Fe)                             | Cd(II)/Pb(II)/Zn(II)/Cr(III) | 155/198/164/173                           | 140    |
|                           | MCNC@Zn–BTC   | Pb(II)                       | 558.66                                    | 141    |
|                           | Fe <sub>3</sub> O <sub>4</sub> @MOF-235(Fe)–OSO <sub>3</sub> H                          | Cd(II)                       | 163                                       | 142    |
|                           | MnFe <sub>2</sub> O <sub>4</sub> @MIL-53@UiO-66@MnO <sub>2</sub> nanomotor              | Pb(II)/Cd(II)                | 1018/440.8                                | 143    |
| Reagent-free regeneration | MIL-121-PVDMBA  | Na(I)                        | 21.2                                      | 28     |
|                           | PSP-MIL-53  | Na(I)                        | 44.6                                      | 144    |
|                           | pNCE/MOF-808  | K(I)                         | 40.7                                      | 145    |
|                           | MOF-808-EDTA  | Na(I)                        | 216                                       | 146    |
|                           | Fe <sub>3</sub> O <sub>4</sub> -MIL-121-NH <sub>2</sub>                                 | Pb(II)                       | 492.4                                     | 132    |
|                           | MIL-121-Ca-Alg  | Cu(II)/Cd(II)                | 204.5/88.7                                | 147    |
|                           | MOF/KNiFC   | Sr(II)                       | 110                                       | 138    |
|                           | HKUST-1-MW@H <sub>3</sub> PW <sub>12</sub> O <sub>40</sub>                              | Pb/Hg/Cd                     | 98.2/0.650/32.5                           | 148    |
| Miscellaneous             | HS-mSi@MOF-5  | Pb(II)/Cd(II)                | 312/98                                    | 149    |
|                           | Melamine-MOFs   | Pb(II)                       | 122                                       | 150    |



## Critical review

A summary of the current state of the art for MOF-based composites, including their compositions, properties, and metal sorption capacities in aqueous solutions is presented in Table 2. In recent years, several studies have been conducted on MOF-based composites for removing heavy metals from water. This review aims to highlight some of the most influential papers in the advancement of MOF-based composite adsorbents, including some of the most recent findings reported in this field to date.

As shown in Table 2, more than a dozen MOF-based composites have been applied successfully to remove metals from water and wastewater, as reported to date. These composites are described in greater detail in the following section.

### Polymer/MOF composite

The polymer refers to a substance or material that contains very large molecules, or macromolecules, composed of a large number of small repeating units, called monomers.<sup>108</sup> They possess unique physical properties due to their large molecular masses compared to small molecule compounds such as toughness, high elasticity, viscoelasticity, and the tendency to form amorphous and semicrystalline structures instead of crystalline structures.<sup>109</sup>

As a result of their combination of highly porous MOFs and flexible polymers, polymer/MOF composites have become increasingly popular.<sup>34,110–112</sup> The realization of polymer/MOF composites which contains the properties of MOFs in a flexible form will allow these materials to be incorporated into industrial applications.<sup>113</sup> In polymer/MOF composites, some important factors include cost, water stability, rapid and selective adsorption, regeneration capability, and adsorption performance across a wide pH range must be considered.<sup>114,115</sup>

As it is shown in Table 2, Queen *et al.* reported water-stable metal-organic framework/polymer composite, Fe-BTC/PDA, that rapidly, selectively removes large amounts of heavy metals like Pb(II) and Hg(II) from real-world water samples.<sup>114</sup> This study treats Fe-BTC with dopamine, which spontaneously polymerizes to polydopamine (PDA) in its pores *via* Fe(III) open metal sites. When tested in high concentrations of organic interferents like humic acid, the material resists fouling and regenerates over many cycles.

This research team developed a general structuring method for preparing MOF/polymer beads in 2020.<sup>116</sup> It was used to create twelve structurally distinct MOFs as well as three MOF-based composites.

A device with a continuous flow was used for the continuous preparation of beads. The tuneable MOF concentration and bead size, as well as the well-preserved crystallinity and surface area, suggest that this method can be easily scaled up. In terms of adsorption properties, one of the resultant beads, known as Fe-BTC/PDA MACPs, demonstrated exceptional performance with ultra-high adsorption of toxic Pb(II) comparable to Fe-BTC/PDA powder,

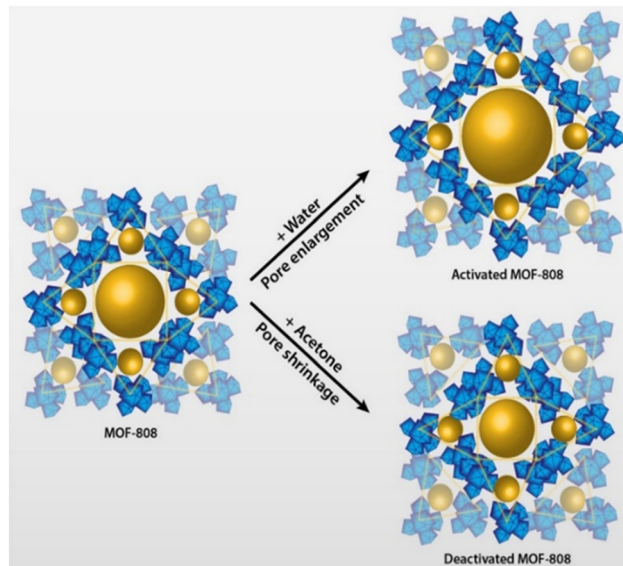


Fig. 4 Hydrate activation of MOF-808 showing pore expansion route with water after vacuum drying and hydrate deactivation of pore shrinkage route with acetone after vacuum drying (reproduced from ref. 121 with permission from American Chemical Society, copyright 2018).

without contaminating the purified water with the catalyst. Significantly, Fe-BTC/PDA MACPs also performed well in extracting Pb from Rhone river water, indicating that they may be applicable in environments containing large amounts of competitive ions. Furthermore, with 498 mg of Pd per gram of composite beads, the beads have one of the highest Pd capacities to date. Additionally, under continuous flow, large amounts of Pd, 7.8 wt%, can be easily concentrated inside the bead, and this value can be easily increased with regenerative cycling.

Polymer/MOF composites can be synthesized in several ways. Top-down approaches to these materials include synthesizing MOFs first and then incorporating them into polymeric materials, and bottom-up approaches involve synthesizing composites as MOF formation occurs. As a result of these approaches, several elegant methods have been developed for the synthesis of polymer/MOF composites, which have brought MOFs closer to becoming useful materials. Besides, there have been many other investigations exploring the possibility of mixing and interacting with these two types of materials.<sup>102</sup> A variety of approaches have been explored for polymer/MOF composites formations, including synthesizing mixed matrix membranes, polymer grafting from MOF particles, polymer grafting through MOFs, polymers templating MOF growth, and MOFs synthesis using polymer ligands.<sup>117</sup> These approaches have utilized a wide range of polymers and MOFs for the integration of polymer/MOF composites to achieve form factors of distinct polymer or MOF characteristics to several desired characteristics.<sup>117,118</sup>

Despite all of the design and preparation challenges in developing polymer/MOF composite adsorbents, some successes have been reported. It has been concluded that polymers with functionalities such as alkyl, hydroxyl, carboxyl,





and amino groups not only are capable of scavenging metals through coordination between heavy metal and functional groups but also provide a pathway to adhere the polymer onto the internal MOF surface which leads to gains extrinsic porosity, resulting in a significantly high adsorption capacity.<sup>114,119,120</sup> Further, no significant uptake of competing metal ions is observed even when interferences, such as  $\text{Na}^+$ , are present at concentrations up to 14 000 times that of  $\text{Pb}^{2+}$ . The material is further shown to be resistant to fouling when tested in high concentrations of common organic interferences, like humic acid, and is fully regenerable over four cycles (Fig. 4). Besides, it was observed that hydrophile polymers can enhance contact between the aqueous phase and substrate, which leads to higher adsorption.<sup>121,122</sup> As reported by Efome *et al.* Fe(III) and Zr(IV) based metal-organic frameworks (MOFs) were woven into polyacrylonitrile (PAN) and polyvinylidene fluoride (PVDF) electro-spun nanofibers to create nanofibrous MOF membranes (NMOM).<sup>122</sup>

Due to the high compatibility between MOF and PVDF nanofibers, no MOF was detected in the permeate after four cycles of filtration and desorption experiments, and more than 90 percent of the NMM hydro-stability of the MOFs, indicate that the NMOMs have the potential to be used for membrane-adsorption-based water treatment. Also, conventional thermal activation of Polymer/MOF composites can lead to a crystal downsizing while 'hydractivation' can cause an expanded MOF with enhanced adsorption potentials (Fig. 4).<sup>121</sup> Moreover, adsorption capacity can be increased by forming complexation between MOF's organic linkers and high heavy metals (Fig. 5),<sup>30</sup> or even between MOF's metal nodes through their terminal hydroxyl groups and high heavy metals.<sup>115</sup> The *in situ* PAN/ZIF-8 filters demonstrated a high adsorption capacity of U(VI) ( $530.3 \text{ mg g}^{-1}$  at  $\text{pH} = 3.0$ ) and an outstanding selectivity toward  $\text{UO}_2^{2+}/\text{Ln}^{3+}$ .<sup>30</sup> The extended X-ray absorption fine structure demonstrated that the adsorption mechanism involved surface complexation between U(VI) and 2-methylimidazole.

Since the surface functionality can be adjusted and the mechanical strength is high, the polymer matrix has proven to be an ideal support for the fabrication of composites as adsorbents, as shown in the papers that examined the combination of MOFs and polymers. The MOF in the composites are separated within the polymer matrix and are less aggregated with one another. Furthermore, the functional groups of the immobilised counterparts are advantageous for metal adsorption. Involved polymers not only serve as supports for the other components, but also as stabilisers, rigid frames, and chelating agents.

### Aerogel/MOF composite

An aerogel is a highly porous amorphous polymer that can be organic, inorganic, or hybrid.<sup>105</sup> Aerogels were made by replacing the liquid in gels with gas while maintaining their porous structures. It must be noted that these synthetic materials are extremely porous (as high as 99.9%) and have

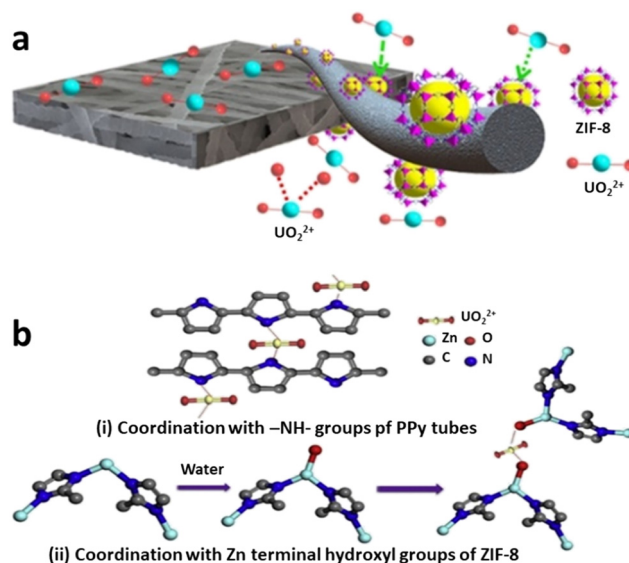


Fig. 5 a) Schematic of the proposed adsorption mechanism of U(VI) ions (reproduced from ref. 30 with permission from American Chemical Society, copyright 2018), and b) proposed mechanisms for the adsorption of U(VI) onto PPy/ZIF-8 through i) MOF's organic linkers, and ii) MOF's metal nodes (reproduced from ref. 115 with permission from Elsevier Inc., copyright 2018).

extremely low densities (as low as  $0.16 \text{ mg cm}^{-3}$ ). Aerogels have high porosities because of their internal solid nanostructure which is made up of cross-linked polymeric nanoparticles with lots of air-filled pores.

Pore sizes that can be tuned are typically in the mesopore range, with a sharp pore size distribution.<sup>151</sup>

Aerogel/MOF composites are synthesized by incorporating the MOF into the aerogel matrix, where the MOF is usually regarded as a dispersed phase, whereas the aerogel matrix is generally considered a continuous phase. Aerogel/MOF composites are capable of taking on various structures that are possible with aerogels, such as monoliths, beads, particles, and fibers. The preparation of aerogel/MOF composites through MOFs incorporation into the aerogel matrix can be accomplished in two ways: (i) direct mixing of pre-synthesised MOFs with gel precursors followed by gelation and drying and, (ii) *in situ* MOFs synthesis inside the aerogel pores.<sup>105</sup> The incorporation approach leads to highly desirable products with hierarchical micro/mesoporosity that can be easily tuned.<sup>137,152</sup> Indeed, aerogels with incorporated MOFs exhibit enhanced mechanical properties.<sup>125</sup> Moreover, the hierarchical structures of aerogel/MOF composites offer excellent opportunities for selective sorption and separation because mesopores and macropores enhance diffusion and mass transfer, while micropores form excellent interactions between host and guest molecules.<sup>152,153</sup>

Aerogels have also been successfully utilised in combination with MOFs to further improve the metal ion adsorption capacity of these materials compared to pristine MOFs. Zhu *et al.* reported synthesis of three different MOF-containing aerogels by combining functional metal-organic



frameworks (ZIF-8, UiO-66 and MIL-100(Fe)) and crosslinkable cellulose nanocrystals (CNCs) to form a stable colloidal suspension in water, and then added to an aqueous solution of crosslinkable carboxymethyl cellulose (CMC).<sup>125</sup> More specifically, crosslinkable celluloses were based on aldehyde modified CNCs (CHO-CNCs) and hydrazide modified CMC (NHNH<sub>2</sub>-CMC) which form hydrazone crosslinks when in contact. It was observed that the aerogel-MOF interaction is primarily due to physical entanglement and van der Waals interactions between MOF particles and aerogel. The aerogels have a hierarchical porous structure with controllable MOF loading up to 50 wt%. The aerogel individually forms colloidal stable suspensions (or solutions) but assembles into covalently crosslinked clusters with entrapped MOFs, when mixed (Fig. 6).

The combination of MOFs, crosslinked clusters, and freeze drying, produced hybrid aerogels with hierarchical pores that remain intact in liquid under compression. The aerogel containing 50 wt% UiO-66 adsorbed 85% of the Cr(vi) after 24 h, whereas aerogels with lower MOF loadings adsorbed 67% (33.3 wt% UiO-66) and 51% (20 wt% UiO-66) of the Cr(vi) due to the lower MOF content. According to UV-vis spectroscopy, aerogels without MOFs (control sample) did not exhibit any removal of Cr(vi) after 24 h. The time dependence of the adsorption was well-fitted to a pseudo-second-order kinetic model with rate constant  $k_2$ , which is the expected diffusion-limited behaviour of MOFs and suggests that the cellulose support is not impeding the access to the MOF pores. In addition to adsorbing large amounts of contaminants, this aerogel could be compressed to squeeze out the water, which always contained a lower concentration of contaminants than the bulk solution (Fig. 7).

One example is the paper reported by Ma *et al.* who developed a feasible method to prepare flexible MOF aerogel through in-site growth of MOF nanoparticles on bacteria cellulose (BC).<sup>126</sup> Due to its large surface area, high porosity and pore accessibility, and the abundance of hydroxyl groups

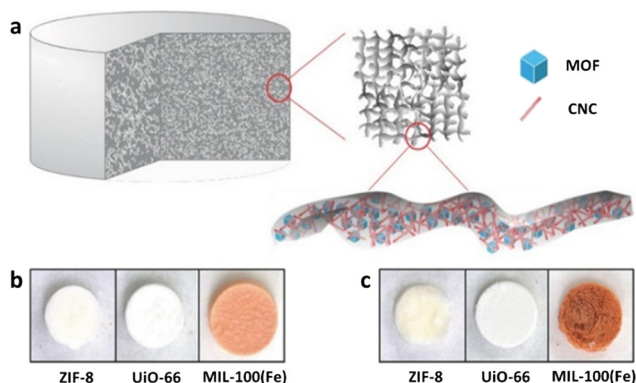


**Fig. 6** a) Schematic of MOF-cellulose hybrid aerogel, b) photographs of CNC-CMC based hybrid aerogels (CNC:CMC:MOF = 1:1:1 by weight), and c) all-CNC based hybrid aerogels (CNC:CNC:MOF = 1:1:1 by weight); aerogels are about 7 mm in diameter and 5 mm in height (reproduced from ref. 125 with permission from Wiley, copyright 2016).

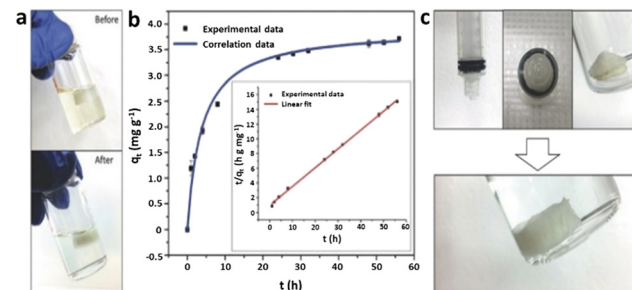


**Fig. 7** a) Photographs of the contaminated aqueous solution before and after adsorbing Cr(vi) in the aerogel with 50 wt% UiO-66, b) the time-dependent adsorption (correlation curve was drawn using the kinetic parameters calculated from the pseudo-second-order model) and pseudo-second-order plots (inset), and c) photographs showing that a wet hybrid aerogel (50 wt% UiO-66) can be incorporated into a syringe and compressed fully by the piston (top left), also shown from the bottom view of the syringe (top middle). When removed from the syringe, the compressed aerogel in the air maintains the shape of the container it was compressed in (top right) but recovers its original shape completely when placed in the solution again (bottom) (reproduced from ref. 125 with permission from Wiley, copyright 2016).

on the surface of BC nanofibers, the BC@ZIF-8 composite aerogel sponge plays a crucial absorbent role in purifying Pb(II) or Cd(II) ions-containing solutions, as determined by adsorption measurements. BC@ZIF-8 composite aerogel sponges with low density (below 0.03 g cm<sup>-3</sup>) are easily separated from solution, which could prevent secondary pollution (Fig. 8).

Besides, the amount of metal ions adsorbed by aerogel/MOF composite is equal to the sum of MOFs and aerogels, indicating that the MOFs are not blocked after aerogels growth (pore accessibility) and consequently they still possess large surface area and high porosity which means they still have good adsorption properties according to Gao *et al.*<sup>123</sup> Furthermore, it was discovered that composite materials made of metal-organic frameworks and cellulose aerogels can be recycled to adsorb Pb(II) and Cu(II) in water after a quick cleaning. Pb(II) adsorbed by UiO-66-NH<sub>2</sub>@cellulose aerogels (CA) had an equilibrium adsorption capacity of 89.40 mg g<sup>-1</sup>, and it was easily reusable for more than five cycles without noticeably losing effectiveness.

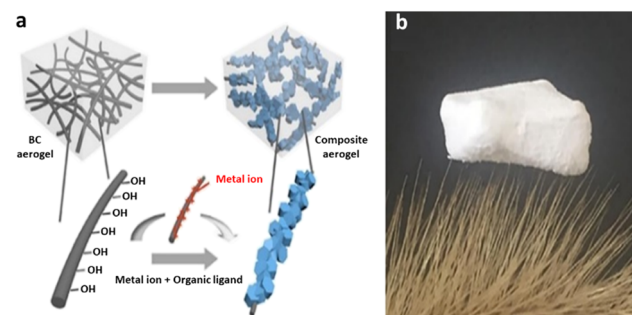


**Fig. 8** a) The fabrication process of BC@MOFs composite aerogels and b) photograph of the lightweight composite aerogels (reproduced from ref. 126 with permission from Elsevier Inc. copyright 2018).



The adsorption capacity can still be greatly improved when compared with a single aerogel or MOF adsorbent. The adsorption capacity can be enhanced using amine groups densely populated on the inner surface of the porous aerogel due to uniquely large specific surface areas and the high density of adsorption sites. As reported in another study by this group, a hybrid cellulose aerogel loaded with 30 wt% zeolitic imidazolate framework-8 (ZIF-8) was synthesised and used for adsorption removal of chromium(vi) from water.<sup>124</sup> ZIF-8@CA's adsorption was modelled as pseudo-second-order kinetic adsorption, and its maximum adsorption capacity for Cr(vi) was calculated to be 41.8 mg g<sup>-1</sup>. When compared to using just CA or ZIF-8, the adsorption capacity was significantly boosted by using both. *N*-Pyridine, which was found in high concentrations on the inner surface of the porous CA, was responsible for the increased adsorption capacity due to its large specific surface area and abundance of adsorption sites.

Moreover, these composites made of aerogels and MOFs can be reused for many cycles and showed good shape stability after recycling. Besides, Compared to just aerogel, incorporation of MOF improved the compressive stress, thermal stability, maximum decomposition temperature ( $T_{\max}$ ), and the complete decomposition temperature ( $T_i$ ) of these composites.<sup>123</sup>

Accordingly, aerogel/MOF composites as an emerging class of composite materials are attracting interest due to their combination of the two materials' superior properties, such as ease of preparation, high surface areas, high pore volumes, high porosities, low densities, controllable micro/mesoporosity ratio, control over morphology, and single-step MOF activation and aerogel formation with enhanced chemical or physical properties that improve the performance in various applications. Moreover, the micro- and mesoporosity of MOFs along with the meso- and macroporosity of aerogels allows MOF/aerogel composites to be made with hierarchically multimodal porous material structures. Aerogel/MOF hybrid sponges with a low density are promising because they can be easily isolated from the solution, thereby reducing the likelihood of secondary pollution.

### Graphene oxide/MOF composites

Graphene oxide (GO) is a two-dimensional carbon material made from oxygen-containing functionalities such as carboxyl, hydroxyl, and epoxy groups that can be regarded as a low-cost and readily available monomolecular layer of graphite.<sup>154</sup> Two major advantages of GO including high atomic density and many surface functional groups make it one of the best additives for other materials. Its physical and chemical properties become interesting and complex due to these groups.<sup>106</sup>

With the combination of GO and MOFs, it is possible to control the distance between the layers of GO, changing the transport and screening of molecules, and providing composites with many potential applications.<sup>106</sup> Apart from

improving physical characteristics, it is also possible to benefit from the desirable properties of both materials types by forming composites of GO and MOF, such as strong hydrophilicity, good chemical stability, high crystallinity, high porosity, and a high specific surface area. Other interesting properties that will result from GO/MOF composite include hydrophilic, antifouling, high-throughput, and high-repulsion properties, as well as efficient, controllable, and low-cost methods of synthesis methods.<sup>106,155</sup> By improving MOF stability under wet conditions, GO/MOF composites have expanded the versatility of MOFs and have led to innovative applications.<sup>156</sup> GO/MOF composites can be prepared in several ways, including *in situ* growth as the simplest method to synthesize the composites, where the MOF precursor is mixed with GO to create the composites.<sup>106</sup> As a result of the epoxy and hydroxyl functional groups on both sides of GO, the composite has bifunctionality and the capacity to interact with MOF metal ions.<sup>157</sup> Since GO has a dense atomic arrangement, it can significantly enhance the dispersion power of GO/MOF materials, which facilitates small molecule adsorption.<sup>106</sup>

In 2017, Rahimi and Mohaghegh reported a hybrid nanocomposite of copper terephthalate metal organic framework (Cu(tpa)) and graphene oxide (GO), Cu(tpa).GO, that the binding mechanism of these two materials was related to both  $\pi$ - $\pi$  packing and hydrogen bonding confirmed by SEM, UV-vis and FT-IR.<sup>129</sup> The prepared adsorbents were assessed for the removal of Mn(II), Cu(II), Zn(II), Cd(II), Pb(II) and Fe(III) metal ions from aqueous synthetic solution and acid mine drainage (AMD) wastewater. The suggested mechanism for the metal ion removal by hybrid nanocomposite is greatly in agreement with the Langmuir and Freundlich adsorption isotherms. Also, the sorption kinetics data confirmed that the sorption reaction obeys the pseudo-second-order kinetics. Interestingly, ion removal results from real sample of mine-related AMD (from Sungun Copper Mine) shows that Cu(tpa)-GO have great potential as an adsorbent for the preconcentration of metal ions.

Another composite of MOFs and graphene oxide was introduced by Yang *et al.* reported in 2017.<sup>128</sup> In this study, the adsorption of U(vi) from an aqueous solution and artificial seawater was reported using GO-COOH/UiO-66 composites which were designed *via* coordination of the carboxyl groups of GO with zirconium ion of UiO-66. Experimental evidence indicates that the removal of heavy metal ions by the composite is based on inner-sphere surface complexation and electrostatic interaction (Fig. 9). The adsorption process closely fitted the Langmuir isotherm model and pseudo-second-order rate equation. In addition, from the XPS and FTIR analyses of the GO-COOH/UiO-66 composites before and after U(vi) adsorption-desorption, the distinctive adsorption capacity was predominately attributed to chelation and a small amount of ion-exchange of U(vi) ions with GO-COOH/UiO-66. The results also indicated that the introduction of GO-COOH didn't change the adsorption performance, but provided more active sites, which improved the adsorption capacity to 1002 mg g<sup>-1</sup> at pH = 8.



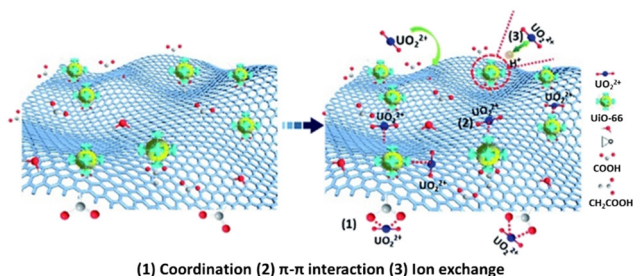


Fig. 9 Proposed mechanisms for the adsorption of  $U(VI)$  onto GO-COOH/UiO-66 composites (reproduced from ref. 128 with permission from Royal Society of Chemistry, copyright 2017).

Han *et al.* reported a facile *in situ* growth synthetic method to achieve cost-effective Graphene oxide (GO)-MIL-101(Fe) (Fe-based metal-organic frameworks (MOFs) with Fe(III) as the metal node and 2-aminobenzene-1,4-dicarboxylic acid as a ligand) sandwich composites towards the  $U(VI)$  capture.<sup>127</sup> Different ratio of GO and MIL-101(Fe) in the composite was tuned through changing the addition amount of GO nanosheets. Adsorption isotherms reveal the much better adsorption performance of the GO15-MIL-101(Fe) (GO dosage is 15 mg) composite than pristine MIL-101(Fe) with larger  $U(VI)$  adsorption capacity and superior reusing ability. The samples kept about 75% of their initial adsorption efficiency even after 8 cycles.

In these three separate studies, it was shown that composite materials of graphene oxide and MOFs are very effective for the adsorption removal of metals from water as they take advantage of both MOF and graphene oxide reactive sites. It showed that the binding mechanism of GO and MOF was related to both  $\pi$ - $\pi$  packing and hydrogen bonding, or in other words the coordination of the functional groups of GO with metal nodes of MOFs.

The special characteristics of GO/MOF composites such as the unique structure formed by  $\pi$ -conjugated networks, binding capacity, and specific functional groups as binding sites considerably influence and enhance the adsorption capacity. The results also indicated that the introduction of GO didn't change the adsorption performance, but provided more active sites, which improved the adsorption capacity. Indeed, the distinctive adsorption capacity was predominately attributed to chelation and a small amount of ion exchange of heavy metal ions with GO/MOF composite.

### Magnetic framework composites

Magnetic metal oxide nanoparticles (MNPs) have excellent magnetic properties that attract a lot of attention.  $Fe_3O_4$ ,  $\alpha$ - $Fe_2O_3$ ,  $\gamma$ - $Fe_2O_3$ ,  $CoFe_2O_4$ ,  $NiFe_2O_4$ ,  $MnFe_2O_4$ ,  $CuFe_2O_4$ , and  $ZnFe_2O_4$  are some of the MNPs that have been synthesized and reported in the literature so far. Despite being easily oxidized by air, MNPs offer a naturally elegant approach to fabricating materials with multiple functions.<sup>158-160</sup> Magnetic framework composites (MFCs) are characterized by outstanding synergistic properties unmatched by the constituent components

individually.<sup>161-163</sup> In addition to offering high surface area, MFCs have enhanced thermal stability.<sup>164</sup>

Furthermore, MFCs with adequate saturation magnetization values can be precisely positioned and easily and quickly separated from complicated matrices with improved efficiency with the use of an external magnet.<sup>165</sup> There is no doubt that magnetic separation is a relatively robust, reliable, highly effective, and easy method for recovering catalysts than conventional techniques, such as filtration and centrifugation, which require considerable time and energy.<sup>166,167</sup> Indeed, the chemical and manufacturing industries place a high priority on the separation and reuse of material to minimise environmental and economic impacts.<sup>140</sup>

Recently, several studies have proved the potential of the combination of MNPs and MOFs for pollutant sequestration. These investigations focused on the adsorption removal of heavy metals from water. The adsorption of heavy metal ions onto magnetic framework composites might be originated from strong surface complex interaction as reported by Alqadami *et al.* (Fig. 10).<sup>134</sup> The Langmuir and pseudosecond-order models accurately described the isotherm and kinetic data. The adsorption of both metal ions by the  $Fe_3O_4@AMCA-MIL53(Al)$  nanocomposite was rapid, and equilibrium was observed for both metal ions within 90 minutes. Under acidic conditions, the leaching studies revealed that  $Fe_3O_4@AMCA-MIL53(Al)$  nanocomposite exhibited significantly enhanced stability. Thermodynamic studies revealed that the adsorption of  $U(VI)$  and  $Th(IV)$  onto the  $Fe_3O_4@AMCA-MIL53(Al)$  nanocomposite was spontaneous and endothermic.

The adsorption of  $Sr(II)$  from aqueous solutions was achieved by Faghihian and Naeimi using a HKUST/potassium nickel hexacyanoferrate composite (HKUST/KNiFC) and a magnetic HKUST/potassium nickel hexacyanoferrate composite system (HKUST/ $Fe_3O_4$ /KNiFC).<sup>138</sup> The adsorption capacity of 110 and 90  $mg\ g^{-1}$  was obtained for the non-magnetized (MOF/KNiFC) and magnetized (MOF/ $Fe_3O_4$ /KNiFC) adsorbents, respectively. The incorporation of KNiFC

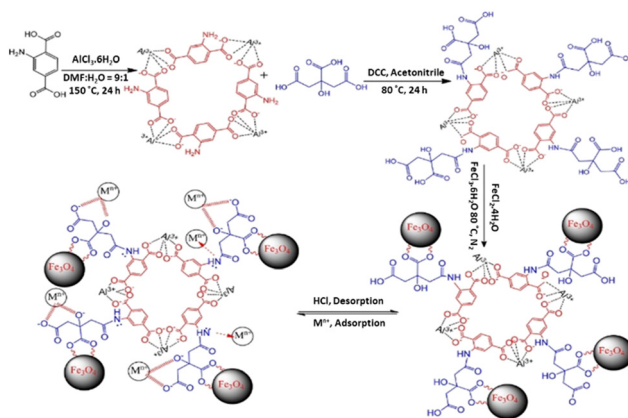
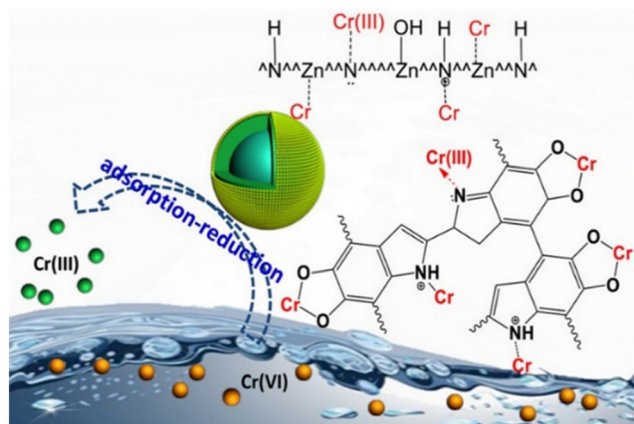


Fig. 10 Synthesis of  $Fe_3O_4@AMCA-MIL53(Al)$  nanocomposite and its adsorption-desorption behaviour for metal ions (reproduced from ref. 134 with permission from American Chemical Society, copyright 2017).



into the MOF structure significantly enhanced its adsorption capacity, which was attributed to its ion-exchange property, while the addition of magnetization facilitated the separation of the adsorbent from the solution. The selectivity of the adsorbent studied in the presence of different cations (Cs(I), Na(I), Mg(II), Ca(II) and Ba(II)) indicated that the tolerance limit was between 50 and 100 mg L<sup>-1</sup>. Within 45 minutes, equilibration was achieved due to the kinetically rapid adsorption process. More than 90% of the adsorbent's original capacity was preserved after regeneration. The endothermic and spontaneous nature of the process was demonstrated by the measured thermodynamic parameters. By examining the magnetic capability of the adsorbent with a vibrating sample magnetometer (VSM), it was determined that the used adsorbent could be separated from the solution by applying an external magnetic field.

In 2018, Huo *et al.* reported on the synthesis of a water stable Fe<sub>3</sub>O<sub>4</sub>@ZIF-8 composite, and its As(III) ion adsorption properties.<sup>136</sup> Powder XRD, SEM, TEM and BET surface areas measurement revealed that as-obtained Fe<sub>3</sub>O<sub>4</sub>@ZIF-8 composites possess core-shell structures (Fe<sub>3</sub>O<sub>4</sub> as core and ZIF-8 as shell) with a high surface area (1133 m<sup>2</sup> g<sup>-1</sup>). The adsorption isotherm is possibly best expressed using the Langmuir model, suggesting that the As(III) uptake on Fe<sub>3</sub>O<sub>4</sub>@ZIF-8 is a monolayer adsorption with a maximum capacity of 100 m<sup>2</sup> g<sup>-1</sup>. Strong surface complex interaction may be the source of this adsorption performance. Statistical analysis of the thermodynamic data showed that the adsorption occurred in an endothermic, spontaneous manner, with entropy increasing as a result. The adsorption kinetics, as determined by batch adsorption experiments, fit pseudo-second-order better ( $R^2 = 0.9881$ ). Additionally, the role of anions in the elimination of As(III) was investigated. The results showed that common anions wouldn't get in the way of metal ion adsorption, with the exception of carbonate and phosphate anions, which could compete with As(III) for adsorptive sites.<sup>134</sup> Furthermore, as reported by Falcaro *et al.*



**Fig. 11** Cr(VI) reduction and immobilisation by the core-double-shell structured magnetic polydopamine@zeolitic imidazolate frameworks-8 microspheres (reproduced from ref. 130 with permission from American Chemical Society, copyright 2017).

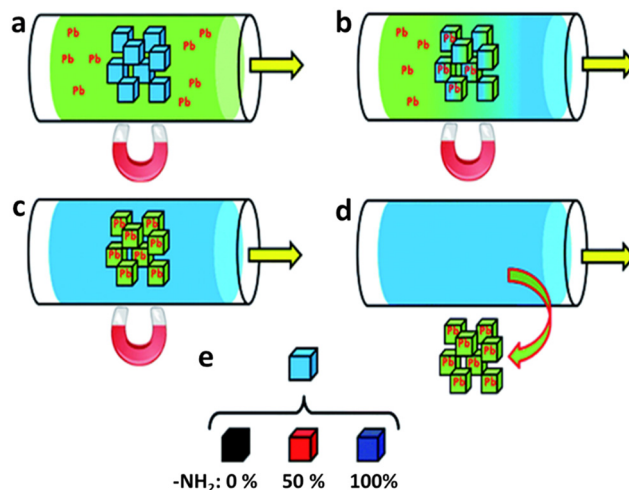


**Fig. 12** Conceptual representation of heavy metal uptake using MFCs: (a) a stream of polluted water passes through a magnetically immobilized MFC filtration zone; (b) the MFCs start to take up the heavy metal (*i.e.* Pb) up to an acceptable level of sequestration (c); (d) removing the magnetic field, it is possible to separate the metal loaded MFCs from the clean water, for secondary extraction and recovery; (e) three types of MFCs were studied, according to the number of amino groups present during MOF synthesis (0%, 50%, and 100%) (reproduced from ref. 132 with permission from Royal Society of Chemistry, copyright 2015).

the fully functionalized magnetic framework composites with amine moieties can show superior performance in Pb(II) adsorption than the materials containing 50% or no amine moieties at all.<sup>132</sup> Heavy metal sequestration capacities in a range of solvents (methanol, DMSO, and water), pH (2, 7, 12), and Pb(II) concentrations were evaluated using composite materials (10–8000 ppm). Pb(II) ions in water were effectively removed by the MIL-53 magnetic composite (up to 492.4 mg g<sup>-1</sup> of composite). The metal-organic framework (MOF) was essential for effective heavy metal uptake, and the magnetic nanoparticles facilitated fast sorbent collection from solution (Fig. 12).

As reported by Ke *et al.*, thiol-functionalized magnetic framework composites through post-synthetic modification with dithioglycol or bismuthiol onto the sites previously occupied by coordinated water molecules can provide extremely high selective adsorption toward specific heavy metals such as for Hg(II) and Pb(II) compared to other ions such as Ni(II), Na(I), Mg(II), Ca(II), Zn(II) and Cd(II) due to the formation of highly stable complexes resulting from the strong interaction between heavy metal ions and sulfur atoms, which act as strong binding sites.<sup>135</sup> Furthermore, due to the presence of the magnetic Fe<sub>3</sub>O<sub>4</sub> core, this adsorbent can be easily recycled. The adsorption kinetics follow the pseudo-second-order rate equation, and Hg(II) and Pb(II) are almost completely removed from the mixed heavy metal ions wastewater (0.5 mM) within 120 minutes.

According to Huang *et al.*, the material exhibited promising kinetics for mercury(II) adsorption, with optimal performance at pH 3. The maximum uptake capacity was



recorded at  $264 \text{ mg g}^{-1}$ , which corresponds to 99.9% adsorption from a solution with a concentration of  $20 \text{ mg L}^{-1}$ , and equilibrium was reached after 10 minutes. Exposure to other metal ions at the same concentrations resulted in only 23% uptake of lead(II) ions and 55% uptake of chromium(III) ions by the framework.<sup>137</sup>

A sulfonate functionalized magnetic framework composites through pre-synthetic modification of organic linker can also enhance the adsorption. Indeed, the electron pair of O and S atoms of sulfonate groups with heavy metal ions can result in the formation of a stable complex which further increases the affinity of the sulfonated group for heavy metal ions (the heavy metal is mainly in the form of positive ion).<sup>142</sup>

Thus, the interaction of MOF and water during heavy metal adsorption from aqueous solutions can produce active sites (e.g., MOF's metal node-OH and protonated N atom groups). These active sites could efficiently adsorb heavy metal. Besides, the magnetic composite and especially amine groups promote the partial reduction of the heavy metal ions (Fig. 11).<sup>130,131</sup>

The adsorption capacities of heavy metals were dimensioned by decreasing the pH values of the aqueous solutions due to protonation of the binding sites on the magnetic framework composites surface, which increased the repulsive forces between the positive ions and adsorbent surface. Furthermore, at lower pH, there was more competition between positive ions and  $\text{H}^+$  for binding sites due to the high contamination of protons. The adsorption capacities increased at higher pH due to the strong attractive forces between the binding sites on the magnetic framework composites surface that are negatively charged and the positive metal ions.<sup>130,131</sup> In some cases, the optimum pH was low, which could be explained by the protonation of amine groups (e.g.,  $=\text{N}-$  and  $-\text{NH}-$  groups) or sulfonic acid groups (e.g.,  $-\text{SO}_3\text{H}$  groups) on magnetic framework composites leading to a high electrostatic interaction between the anionic species metal ions and magnetic framework composites surface.<sup>140,142</sup>

Moreover, the adsorption capacity of the composite was significantly improved relative to that of MNPs in isolation.<sup>133,141</sup>

Despite the necessity of MOFs for successful heavy metal adsorption, the addition of MNPs may have reduced the performance of the material. However, by applying an external magnetic field to the magnetic nanoparticles, the adsorbent can be quickly collected from the solution, and the regenerated composites retain nearly all of their original capacity.

Based on experimental evidence presented here, magnetic composites have many benefits over other solid-phases, including a low time-consumption due to the magnetically-assisted separation of the adsorbent, high enrichment capacity, significantly improved stability under acidic conditions, stable performance in consecutive cycles, low limit of detection, and high enrichment factor.

## Reagent-free regeneration composites

Adsorbents are commonly single-use or regenerated in conditions away from the adsorption environment. Typically, this is achieved with acids or bases to remove adsorbed species by ion exchange. While in some cases regeneration and its associated change of desorption are not desired, such as in radioactive metal removal, adsorption concentration of metals such as lithium are desirable. Recent work has demonstrated MOF-composites that are regenerated by thermal, light, and magnetic induction stimuli. Such examples focus on adsorbent regeneration rather than adsorption reveals ways for MOFs to be incorporated as smart materials.

Thermal responsive polymers undergo configurational changes at a critical temperature, such as poly(*N,N*-dimethyl-4-vinyl), (PDMVBA) or poly(*N*-isopropylacrylamide) (PNIPAM) that undergo a hydrophilic–hydrophobic transition at  $80 \text{ }^\circ\text{C}$  or  $45 \text{ }^\circ\text{C}$ , respectively. This property was exploited for temperature swing adsorption demonstrations with PDMVBA-MIL-121 and pNCE-PNIPAM-MOF-808 composites that adsorbed alkali metals.<sup>28,145</sup> In the second case, a  $\text{Na}^+$  and  $\text{K}^+$  selective benzo-18C6 moiety allowed for the purification of  $\text{Li}^+$  in the filtrate.

Light-responsive polymers containing moieties such as spiropyrans and azobenzene undergo reversible bond cleavage or isomerisation, respectively, to modify the properties of the overall material. PSP-MIL-53 adsorbed salts broadly from brackish water and remarkably desorbed near totally within 4 min under 1 sun irradiation.<sup>144</sup> This sunlight swing adsorption is due to the formation of a positive–negative charge pair by UV cleavage of a spiro group, while under visible light it reforms the C–O bond and becomes covalent.

MIL-121 and similar thermal-breathing MOFs are being actively investigated to undergo reagent-free regeneration by temperature change. The  $\text{pK}_a$  of COOH groups changes from carboxylate-dominated to carboxylic acid-dominated when the temperature increases from  $25 \text{ }^\circ\text{C}$  to  $80 \text{ }^\circ\text{C}$  at neutral pH. This can be exploited to utilise low volumes of hot water to regenerate COOH-containing MOFs, such as in recent work combining MIL-121 and calcium alginate to form macroscopic beads for ease of handling, removing Cd(II) and Cu(II) with a decent capacity of  $204.5 \text{ mg g}^{-1}$  and  $88.7 \text{ mg g}^{-1}$ , respectively.<sup>147</sup>

While composites with magnetic nanoparticles commonly adsorb metals and are then magnetically collected, as described previously, their use in induction heating to release adsorbates has yet to be explored thoroughly. The singular example, IOMN-MIL-53-NH<sub>2</sub>, adsorbed Pb(II) under a variety of conditions and then could release 60% of adsorbed Pb(II) 3× faster under induction heating than under room temperature.<sup>132</sup> Such remote heating does not require challenging geometries such as sunlight or heating and pumping of thermally conductive fluid.

## Miscellaneous

There are other materials which in combination with MOFs provide effective removal of metals from water. In 2013, Zou



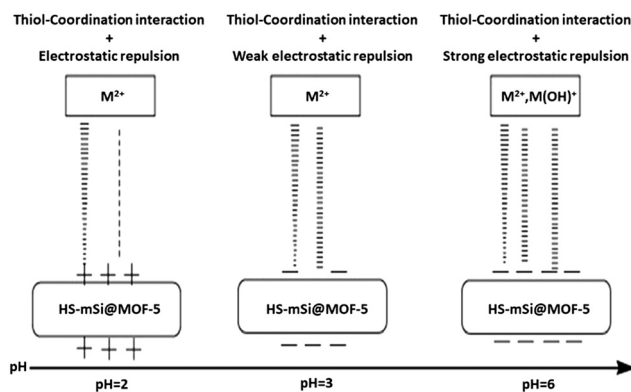


Fig. 13 A plausible mechanism of heavy metals adsorption over HS-mSi@MOF-5 (reproduced from ref. 149 with permission from Elsevier Inc., copyright 2016).

*et al.* developed HKUST-1 composite with a Keggin-type polyoxometalate, HKUST-1-MW@H<sub>3</sub>PW<sub>12</sub>O<sub>40</sub>.<sup>148</sup> This MOF composite was used for adsorption removal of heavy metals in water, the adsorption capacity of 98.18 mg g<sup>-1</sup> for Pb<sup>2+</sup> and 32.45 mg g<sup>-1</sup> for Cd<sup>2+</sup> was observed while no Hg<sup>2+</sup> uptake occurred. The adsorption processes studied involve interactions lying between chemical and physical adsorption, although the main type of adsorption of heavy metal ions is chemical adsorption.

Alkordi *et al.* reported a one-pot synthesis for constructing a metal-organic framework (MOF) composite of the amino-derivative Zr carboxylate and silica gel (UiO-66-NH<sub>2</sub>@silica).<sup>168</sup>

As a porous solid support, silica gel was used to improve column packing efficiency and increase sorbent-solute contact time. The control experiment conducted on bare silica established unequivocally the role of the amino-functionalized MOF as the ion-exchange component in the novel composite. This composite produces a column with exceptional hexavalent chromium uptake (Cr<sub>2</sub>O<sub>7</sub><sup>2-</sup> uptake of 277.4 mg g<sup>-1</sup>). Remarkably, this ion exchange column can remove Cr(vi) ions even in the presence of competing anions such as chloride, bromide, nitrate, and sulphate, indicating its potential for use in municipal and industrial waste water treatment. In order to examine column recyclability, a column subjected to a 6 ppm dichromate solution was regenerated eight times consecutively, with acid and water washes between cycles, and showed no decline in Cr(vi) capture activity over the range of cycles examined.

Removal of metals highly depends on pH, the acidic conditions increase competition between the metal ions and a proton, whereas there is precipitate formation within the solution at pH > 6. The possible mechanisms between HS-mSi@MOF-5 and lead or cadmium ions are proposed in Fig. 13.

Melamine-modified metal-organic frameworks (melamine-MOFs) were reported by Yin *et al.* in 2018 for the removal of heavy metal Pb(II) from a low-salt solution.<sup>150</sup> According to time-dependent density function theory (TD-

DFT) calculations, there were charge transfer and orbital switching between the melamine and MOFs. Also, FT-IR and thermal gravimetric analysis (TGA) indicated the melamine was not physically mixed with the MOFs and there is a chemical reaction. The removal of Pb(II) occurred *via* the coordination interaction between the amino groups (-NH<sub>2</sub>) and lead ions. Its maximum adsorption was recorded at a pH of 6 (about 205 mg g<sup>-1</sup>), and the adsorption rate agreed with a pseudo-second-order equation.

The self-propel of a magnetic MOF composite was achieved by utilizing a nanomotor based on the degradation of MnO<sub>2</sub> peroxide. MnFe<sub>2</sub>O<sub>4</sub>@MIL-53@UiO-66@MnO<sub>2</sub> nanomotor concept eliminates the need for mechanical or magnetic stirring, which is usually required to maintain high contact with adsorbents. Due to the incorporation of magnetic MnFe<sub>2</sub>O<sub>4</sub>, the post-adsorption collection was also demonstrated to be easy. *In situ* remediation could benefit from this concept, as adsorbents can move within contaminated water without external aid.

## Mechanisms of metal ions removal from water using MOF-based composite adsorbents

Adsorption mechanism understanding is difficult, but it's worth it since it leads to better adsorbent design and more optimal adsorption and desorption conditions that boost adsorption's practicality. Adsorption is an exothermic process with three distinct mechanisms: physisorption, chemisorption, and ion exchange.<sup>169,170</sup> It is essential to highlight that the MOF composites' ability to absorb metal ions is proportional to the strength of their adsorption mechanisms.<sup>31</sup> Moreover, in order to get insight into the adsorption mechanisms, there is a standard experimental procedure to analyse the adsorption isotherm and kinetic.<sup>61,64,67,149,171</sup> Physical adsorption (physisorption or adsorptive adsorption) is distinguished by weak intermolecular interactions that are reversible. It specifies a surface bond between the adsorbent and the adsorbate that does not disturb their respective electronic orbitals. It consists of diffusion, hydrogen bond, Van der Waals interactions, and hydrophobic interactions ( $\pi$ - $\pi$  interactions and Yoshida interactions).<sup>172-174</sup> The adsorption process is influenced by diffusion, and the kinetic patterns can be examined using intraparticle diffusion modelling. In the intraparticle diffusion model, the number of straight lines normally represents distinct adsorption methods through the intraparticle diffusion constant and the constant representing the boundary layer effect.<sup>149</sup> The hydrogen bond is defined as bonding between organic molecules that include hydrogen bonded to an electronegative element that withdraws electrons from the H atom; hence the H atom becomes electron-deficient owing to the lack of electron shielding, and the metal ion contains a pair of lone electrons.<sup>175</sup> The Van der Waals force is a basic adsorption



mechanism applicable to all adsorbates when the surface area or porosity is considered. MOF composites are differentiated by their high surface area and considerable porosity, which enables the significant selective adsorption of metal ions.<sup>70,176,177</sup> The term “hydrophobic interactions” refers to the bonding between nonpolar molecules in MOF composites and non-polar adsorbates which includes  $\pi$ - $\pi$  interactions between two unsaturated (poly)cyclic molecules (aromatic rings), and Yoshida interactions between the OH groups and the aromatic rings.<sup>178</sup> For example, Fang *et al.* found that after capturing Co(II), the pore size of a PCN-100 framework shrank and the density rose, indicating that the PCN-100 had successfully caught the Co(II) ions through the Van der Waals force.<sup>70</sup> Chemical adsorption (chemisorption or reactive adsorption) is characterised by irreversible chemical interactions involving electronic orbitals and valence forces between the adsorbent and adsorbate. It produces a surface bond between the adsorbent and the adsorbate that induces a change in their respective electronic orbitals. It includes electrostatic interaction, coordination interaction, chelation, covalent bonding, and Lewis acid–base interaction.<sup>31,172,179</sup> Electrostatic interaction describes the interaction of charged MOF composites with the oppositely charged metal ions which is governed by the MOF composites' surface charges. Both the pH of the aqueous solution and the grafting of certain species onto MOF composites can cause a shift in the surface charge, leading to subsequent protonation or deprotonation. Both the surface potential of MOFs (defined as the point of zero charge, pzc) and the metal ions play a role in the adsorption of metal ions by MOF composites. Typically, the solution pH has a substantial effect on the divalent metal ions owing to the formation of high quantities of hydrated hydrogen ions at low pH. It is expected that in an acidic solution (pH < pzc), positively charged metal ions would compete with hydrated hydrogen ions for accessible adsorption sites, eliminating the electrostatic attraction between MOF composites and metal ions. Instead, the MOF composites are negatively charged and attract metal ions electrostatically when the solution is basic (pH > pzc).<sup>31,178</sup>

The coordination interaction occurs when atoms in MOF composites are in a semi-constrained state and coordinate with metal ions on the surface. It typically happens between MOF composites with different functional groups, such as amino group ( $-\text{NH}_2$ ), carboxyl group ( $-\text{COOH}$ ), and thiol group ( $-\text{SH}$ ), and metal ions, showing that functional groups outweigh the inherited adsorption characteristics.<sup>64,180</sup> Chelation refers to the formation of numerous coordination bonds between polydentate organic molecules and a metal ion, which ultimately results in the sequestration of the metal.<sup>51,181–184</sup>

The formation of covalent bonds takes place when atoms of MOF composites and atoms of metal ions share pairs of electrons with one another.<sup>40,42,133,185–187</sup>

Reaction between basic sites in MOF composites (acting as electron pair donors) and acid sites in metal ions (acting as

electron pair acceptors) is the basis of the Lewis acid–base interaction.<sup>53,149,188</sup> For example, Wang *et al.* observed that a substantial new band, the Zr–O–As group, formed after using UiO-66 for adsorbing As(v) in an aqueous solution, showing that As was bound to the adsorbent due to covalent bonding formation.<sup>40</sup> Luo *et al.* developed an amino-functional MIL-101(Cr) which interacted with Pb(II) ions as a result the coordination interaction between MOF-( $\text{NH}_2$ )<sub>3</sub><sup>3+</sup> (resulting from a significant number of free hydrogen ions in the water mixed with the  $-\text{NH}_2$  groups) and Pb(II) ions when the pH of the solution was acidic.<sup>64</sup> According to Wang *et al.*, the adsorption capacities of Cr(VI) (in the form of  $\text{Cr}_2\text{O}_7^{2-}$ ), Cu(II), and Ni(II) in the chitosan/UiO-66 composite are a result of Lewis acid–base interactions between high oxidation state metal ions and oxygen atoms or the  $\text{NH}_2$  groups of the linkers at lower pH values.<sup>120</sup> Han *et al.* demonstrated, based on the adsorption isotherms of graphene oxide-MIL-101(Fe) composite, that the adsorption performance by addition of GO is much greater than pristine MIL-101(Fe) with U(VI) ions owing to the synergistic effects of GO and MIL-101(Fe) octahedrons. The removal of U(VI) by the composite seems to rely on electrostatic interaction, according to experimental findings.<sup>127</sup> The melamine-MOFs described by Yin *et al.* for the removal of Pb(II) ions from a low-salt solution demonstrated that the removal of Pb(II) occurs through coordination interaction between the amino groups ( $-\text{NH}_2$ ) and lead ions. Maximum adsorption was seen at a pH of 6, and the adsorption rate matched a pseudo-second-order rate model.<sup>150</sup>

Ion exchange adsorption is complex reversible process, stoichiometric, and electrostatic. This is achieved by exchanging the surface ions of the MOF composites for metal ions. The process of adsorption results in electro-neutrality because the ion exchanged during adsorption is released into the surrounding environment. Ion-exchange can be broken down into three categories of cation exchange, anion exchange, and reversible exchange of ions. The cation exchange contains positively charged ions and replaces cations; anion exchange owns negatively charged ions and replaces anions; and reversible exchange of ions consists of the exchange of a charge ion for a similarly charged ion attached to MOF composites.<sup>81,83,189–194</sup> As an example, Faghihian and Naeimi used a HKUST/potassium nickel hexacyanoferrate composite (HKUST/KNiFC) and a magnetic HKUST/potassium nickel hexacyanoferrate composite system (HKUST/ $\text{Fe}_3\text{O}_4$ /KNiFC) to adsorb Sr(II) from aqueous solutions. Due to the ion-exchange ability of this chemical, the incorporation of KNiFC into the MOF structure considerably enhanced its adsorption capacity, while magnetisation aided the separation of the utilised adsorbent from the solution.<sup>138</sup>

Adsorption isotherms data was often fit using the Langmuir isotherm model for homogeneous surfaces and the Freundlich isotherm model for heterogeneous surfaces.<sup>31</sup> Based on the findings resulted from literatures presented in the Table 2, the pseudo-second-order rate models have been shown to have greater correlation coefficients with experimental data than pseudo-first-order rate models, suggesting a better match with





adsorption kinetics data. Moreover, it was discovered that the adsorption isotherms of metal ions by MOF composites are more accurately represented by the Langmuir isotherm model. The Langmuir isotherm model is a kind of chemical adsorption that is thought to be more stable and have a higher capacity than physical adsorption or ion exchange. It is important to note that the assumption behind the pseudo-second-order rate model is that chemical adsorption alone is the rate-limiting step in the adsorption process. Metal ion adsorption on MOF composites in aqueous solutions could be predominantly controlled by chemical adsorption, as shown by the agreement of the Langmuir isotherm model with the adsorption isotherms and kinetic data with the pseudo-second-order rate model.

On the other hand, by comparing results, it was found out that the MOF composites' adsorption mechanisms do not function individually, but rather have a synergistic effect that leads to a higher adsorption capacity. In metal ion adsorption employing MOF composites, it is possible to have a combination of the same kind of mechanisms or a combination of distinct types of mechanisms. For example, Vu *et al.* showed there are two type of chemical adsorption mechanisms of As(III) using MIL-53(Fe). It was revealed that at a pH < 6, the central ions of MIL-53(Fe), Fe<sup>3+</sup>, had an electrostatic interaction with H<sub>2</sub>AsO<sub>4</sub> in solution. The second interaction occurred between the Lewis acid central Fe<sup>3+</sup> and the Lewis base H<sub>2</sub>AsO<sub>4</sub>.<sup>195</sup> As another example, Zhang *et al.* showed there are two type of chemical adsorption mechanisms and a physical adsorption mechanism contributed in the adsorption of Pb(II) and Cd(II) ions onto HS-mSi@MOF-5. Pseudo-second-order rate model was found to suit the adsorption kinetics, while the Langmuir isotherm model was found to fit the adsorption isotherm. Besides, the adsorption capacities of HS-mSi@MOF-5 increased with increasing pH, and the greatest adsorption capacities were found at pH = 7, suggesting that electrostatic interaction is the predominant factor enabling the adsorption. Besides, the Lewis acid-base interaction in HS-mSi@MOF-5 caused the soft acid Pb(II) and boundary acid Cd(II) ions to preferentially connect with the thiol group as a sort of soft base. Metal ions are removed by a three-step diffusion process, which was discovered to be the other adsorption mechanism.<sup>149</sup> Or as another example, Yang *et al.* reported a GO-COOH/UiO-66 composites for adsorption of U(VI) from an aqueous solution and artificial seawater. The adsorption process closely fitted the Langmuir isotherm model and pseudo-second-order rate model. The distinctive adsorption capacity was predominately attributed to chelation and a small amount of ion-exchange of U(VI) ions with GO-COOH/UiO-66 which was confirmed using XPS and FTIR analyses.<sup>128</sup>

## Post-treatment of MOFs after adsorption

Typically, disposal of the undesirable concentrated metal solution after ion exchange is beyond the scope of

articles; however, in light of the growing interest in the circular economy, we have attempted to address this topic. In the case of pure MOFs, dispersion in water enables rapid adsorption properties *via* extensive contact with the outer surface. However, incomplete collection of MOFs results in secondary contamination of MOF nanoparticles, whereas dissolving MOFs releases the constituent node and linkers.<sup>196–199</sup> Metals absorbed by MOFs are also concentrated and may cause solid pollution. The discussed MOFs are typically regenerated in a new location using a chemical regenerant, allowing for multiple uses of the MOF sorbent.<sup>200</sup> At the end of their useful lives, MOFs can be saturated and disposed of as nanoparticle waste and heavy metal liquid waste streams, according to local regulations. As the production scale of MOFs approaches multiple kilograms, green-synthetic techniques, formation into composites, and reagent-free regeneration will help MOFs surpass existing broad-spectrum adsorbents.

As MOF adsorption percentages approach 100% at ppb concentrations, recycling of adsorbed metals is gaining popularity. The economic and industrial value of recovering precious metals such as gold and platinum from diluted waste is significant.<sup>116</sup> These regenerated composites can be utilised repeatedly. In these instances, the benefit of a highly selective MOF, along with a high adsorption capacity and rapid kinetics, may provide a financial incentive. Before the general desalination process, desalination plants could utilise adsorption columns to extract trace amounts of gold from seawater.

The variety of MOF-based composites also allow for further advantages post treatment. The combination of polymers, aerogel, and GO makes it possible to create macroscale materials with a reduced rate of attrition. This reduces secondary environmental pollution caused by the unintended release of MOF nodes and linkers into water. By undergoing selective ion exchange, the polymer/MOF composites described in Table 2 are regenerable in acidic environments. Magnetic attraction similarly reduces the loss of suspended MOF in magnetic framework composites. Furthermore, magnetic separations can be performed with little concern for the surface charge of loaded adsorbents, pH, or ionic concentration of the adsorption solution. For maximum success, good adhesion between nanoparticles and MOF is required, as directed by chemical interactions and careful synthetic conditions. Reagent-free regeneration will significantly reduce the lifetime impact of the MOF adsorbent, a promising field due to the high potential for utilising sustainable regeneration. Utilizing hot water or sunlight that is available through solar concentrators can also enable on-site regeneration and application in regions lacking significant infrastructure (roads/vehicles to transport chemicals, chemical manufacturing and storage, and training for handling chemicals). Green treatments and synthetic techniques, such as framework reassembly, may



offer additional advantages over conventional metal adsorbents.<sup>201,202</sup> In this way, MOFs can be prepared and recycled into new MOFs with minimal additional material. However, future research should place more emphasis on the regeneration and reuse of MOF-based adsorbents.

## Comparison and evaluation of the MOF-based composite adsorbents

In order to prepare MOF-based composite adsorbents with a variety of structures, morphologies, and applications, several distinct composites through the integration of MOFs with a variety of functional materials have been developed. MOF-based composites not only have the dual benefits of MOF (porous structure, chemical versatility, structural tailorability) and various types of functional materials (unique selectivity, magnetic properties, and mechanical strength), but they can also take use of the synergistic impact between the two components to further boost the benefits. As a result of the synergistic effect, new physical and chemical properties can be elicited in MOF-based composites. All of the composites have been examined and analysed from all of the different perspectives, including the compositions and the methodologies, and weighing their strengths and flaws in order to give you a clearer picture.

There are several methods for preparing a MOF-based composite, including encapsulation, impregnation, infiltration, solid grinding, coprecipitation, *etc.* Different kinds of preparation methods may provide distinct characteristics in MOF-based composites, hence expanding their range of potential applicability. The increased porosity of MOF-based composites and their associated higher adsorption capacity is one of their most notable enhancements. Some MOF-based composites demonstrate unique functionality and enhanced practical applications. Some others exhibit structural modifications and enhanced kinetics in the synthesis of MOFs, as well as imparting new features that increase the adaptability of the materials in various ways which improve the versatility of the materials in different aspects.

The polymer/MOF composites possess intriguing features such as macro-shaping with robust structure and hierarchically porous without significantly altering the porosity. The generally cheap cost and ease of preparation, as well as the potential of a vast MOF selection, give this category of composites a very high importance. However, polymers may clog the pores of MOFs and cannot withstand very high temperatures, which are problems for this category of composites. The aerogels/MOF composites higher surface area, as well as macro-shaping and the potential of a broad range of MOF selection, are interesting properties that set this group apart. However, aerogels/MOF composites have disadvantages, including poor mechanical qualities owing to aerogels' very high porosities and the absence of holes in the micropore area. The graphene oxide/MOF composites presented enhancements to the specific surface area and

active sites of MOF and boosts the structural stability. Hierarchically porous, simple production, and higher adsorption capacity are further noteworthy characteristics of this class of composites. Nevertheless, this class suffers from lack of shaping and reagent-free regeneration. The magnetic framework composites' notable properties include a better adsorption capacity and faster separation. Constraints on this category of composites include a lack of shapeability, a restricted selection of MOFs, and poor base stability. The reagent-free regeneration composites provide broad adsorption and easy regeneration but suffer from difficult synthesis, limited shaping, limited investigation scope, and high cost.

## Conclusions and outlook

Pollution of surface and groundwater by metals has disturbing public health consequences and rectification of this situation is a significant challenge. A wide range of materials has been reported for decontamination of water from metals. Water-stable metal-organic frameworks with high surface area and tuneable pores have been shown that they can play a role in the removal of metals from water, however, a 'bare' MOF is difficult to process and regenerate. MOF composites overcome processing and recycling issues as they can be shaped into structures that retain porosity and adsorption performance with improved physical properties. Magnetic particles, different types of polymers, and graphene oxide are some materials that have been made into composites with MOFs to manipulate functionality, porosity, stability, and separation techniques. The composites have also been able to improve the electric/thermal/magnetic properties and be used effectively in the adsorption removal of metals from water.

Given the current interest from both academia and industry, the wide range of applications for MOF-based composite adsorbents, and their diverse types and synthesis strategies, it is anticipated that the next few decades will be flooded with a vast amount of research, especially with regard to recyclability, regeneration, upscaling and stability. In addition, future research should concentrate on minimising manufacturing costs by relying on straightforward and eco-friendly methods for creating MOF-based composite adsorbents. Future studies should also place a greater emphasis on the development of MOF-based composite adsorbents techniques, adsorption capacity, and adsorption selectivity with a minimal influence on environmental balance. Moreover, in the composite process, the interface compatibility of materials should be considered, and the diffusion and mass transfer rate, thermal stability, water stability, and mechanical stability should be targetedly enhanced.

## Conflicts of interest

There are no conflicts to declare.



## References

- 1 A. J. Howarth, Y. Liu, J. T. Hupp and O. K. Farha, Metal-organic frameworks for applications in remediation of oxyanion/cation-contaminated water, *CrystEngComm*, 2015, **17**, 7245–7253.
- 2 P. B. Tchounwou, C. G. Yedjou, A. K. Patlolla and D. J. Sutton, *Molecular, Clinical and Environmental Toxicology: Volume 3: Environmental Toxicology*, Springer, 2012, pp. 133–164.
- 3 U. Förstner, W. Salomons and P. Mader, *Heavy Metals: Problems and Solutions*, Springer, 1995, pp. 33–52.
- 4 A. G. Chmielewski, T. S. Urbański and W. Migdał, Separation technologies for metals recovery from industrial wastes, *Hydrometallurgy*, 1997, **45**, 333–344.
- 5 US Environmental Protection Agency, *Drinking water contaminants*, <https://water.epa.gov/drink/contaminants/index.cfm>.
- 6 A. Dabrowski, Z. Hubicki, P. Podkościelny and E. Robens, Selective removal of the heavy metal ions from waters and industrial wastewaters by ion-exchange method, *Chemosphere*, 2004, **56**, 91–106.
- 7 F. Fu and Q. Wang, Removal of heavy metal ions from wastewaters: A review, *J. Environ. Manage.*, 2011, **92**, 407–418.
- 8 G. Blandin, A. R. D. Verliefe, J. Comas, I. Rodriguez-Roda and P. Le-Clech, Efficiently combining water reuse and desalination through forward osmosis—reverse osmosis (FO-RO) hybrids: A critical review, *Membranes*, 2016, **6**, 37.
- 9 S. Li, Y. Chen, X. Pei, S. Zhang, X. Feng, J. Zhou and B. Wang, Water purification: Adsorption over metal-organic frameworks, *Chin. J. Chem.*, 2016, **34**, 175–185.
- 10 M. Hua, S. Zhang, B. Pan, W. Zhang, L. Lv and Q. Zhang, Heavy metal removal from water/wastewater by nanosized metal oxides: A review, *J. Hazard. Mater.*, 2012, **211**, 317–331.
- 11 R. Taman, M. Ossman, M. Mansour and H. Farag, Metal oxide nano-particles as an adsorbent for removal of heavy metals, *J. Adv. Chem. Eng.*, 2015, **5**, 1–8.
- 12 L. Z. Lee, M. A. A. Zaini and S. H. Tang, *Handbook of ecomaterials*, Springer, 2019, pp. 469–494.
- 13 A. Deliyanni Eleni, Z. Kyzas George, S. Triantafyllidis Kostas and A. Matis Kostas, Activated carbons for the removal of heavy metal ions: A systematic review of recent literature focused on lead and arsenic ions, *Open Chem.*, 2015, **13**, 699–708.
- 14 U. Wingenfelder, C. Hansen, G. Furrer and R. Schulin, Removal of heavy metals from mine waters by natural zeolites, *Environ. Sci. Technol.*, 2005, **39**, 4606–4613.
- 15 S. E. Bailey, T. J. Olin, R. M. Bricka and D. D. Adrian, A review of potentially low-cost sorbents for heavy metals, *Water Res.*, 1999, **33**, 2469–2479.
- 16 M. I. Inyang, B. Gao, Y. Yao, Y. Xue, A. Zimmerman, A. Mosa, P. Pullammanappallil, Y. S. Ok and X. Cao, A review of biochar as a low-cost adsorbent for aqueous heavy metal removal, *Crit. Rev. Environ. Sci. Technol.*, 2016, **46**, 406–433.
- 17 H.-C. Zhou, J. R. Long and O. M. Yaghi, Introduction to metal-organic frameworks, *Chem. Rev.*, 2012, **112**, 673–674.
- 18 H. Furukawa, K. E. Cordova, M. O’Keeffe and O. M. Yaghi, The chemistry and applications of metal-organic frameworks, *Science*, 2013, **341**, 1230444.
- 19 I. Ihsanullah, Applications of MOFs as adsorbents in water purification: Progress, challenges and outlook, *Curr. Opin. Environ. Sci. Health*, 2022, **26**, 100335.
- 20 H. Li, M. Eddaoudi, T. L. Groy and O. M. Yaghi, Establishing microporosity in open metal-organic frameworks: Gas sorption isotherms for Zn(BDC) (BDC=1,4-benzenedicarboxylate), *J. Am. Chem. Soc.*, 1998, **120**, 8571–8572.
- 21 B. F. Hoskins and R. Robson, Infinite polymeric frameworks consisting of three dimensionally linked rod-like segments, *J. Am. Chem. Soc.*, 1989, **111**, 5962–5964.
- 22 N. Bakhtiari and S. Azizian, Adsorption of copper ion from aqueous solution by nanoporous MOF-5: A kinetic and equilibrium study, *J. Mol. Liq.*, 2015, **206**, 114–118.
- 23 A. Demessence, D. M. D’Alessandro, M. L. Foo and J. R. Long, Strong CO<sub>2</sub> binding in a water-stable, triazolate-bridged metal-organic framework functionalized with ethylenediamine, *J. Am. Chem. Soc.*, 2009, **131**, 8784–8786.
- 24 H. Zhang, J. Hou, Y. Hu, P. Wang, R. Ou, L. Jiang, J. Zhe Liu, B. D. Freeman, A. J. Hill and H. Wang, Ultrafast selective transport of alkali metal ions in metal organic frameworks with subnanometer pores, *Sci. Adv.*, 2018, **4**, 1–8.
- 25 Y. Huang, X. Zeng, L. Guo, J. Lan, L. Zhang and D. Cao, Heavy metal ion removal of wastewater by zeolite-imidazolate frameworks, *Sep. Purif. Technol.*, 2018, **194**, 462–469.
- 26 T. Xu, M. A. Shehzad, D. Yu, Q. Li, B. Wu, X. Ren, L. Ge and T. Xu, Highly cation permselective metal-organic framework membranes with leaf-like morphology, *ChemSusChem*, 2019, **12**, 2593–2597.
- 27 J. Dechnik, J. Gascon, C. J. Doonan, C. Janiak and C. J. Sumbly, Mixed-matrix membranes, *Angew. Chem., Int. Ed.*, 2017, **56**, 9292–9310.
- 28 R. Ou, H. Zhang, J. Wei, S. Kim, L. Wan, N. S. Nguyen, Y. Hu, X. Zhang, G. P. Simon and H. Wang, Thermoresponsive amphoteric metal-organic frameworks for efficient and reversible adsorption of multiple salts from water, *Adv. Mater.*, 2018, **30**, 1802767.
- 29 N. D. Rudd, Y. Liu, K. Tan, F. Chen, Y. J. Chabal and J. Li, Luminescent metal-organic framework for lithium harvesting applications, *ACS Sustainable Chem. Eng.*, 2019, **7**, 6561–6568.
- 30 C. Wang, T. Zheng, R. Luo, C. Liu, M. Zhang, J. Li, X. Sun, J. Shen, W. Han and L. Wang, In situ growth of ZIF-8 on PAN fibrous filters for highly efficient U (VI) removal, *ACS Appl. Mater. Interfaces*, 2018, **10**, 24164–24171.
- 31 J. Wen, Y. Fang and G. Zeng, Progress and prospect of adsorptive removal of heavy metal ions from aqueous solution using metal-organic frameworks: A review of studies from the last decade, *Chemosphere*, 2018, **201**, 627–643.



- 32 M. Feng, P. Zhang, H.-C. Zhou and V. K. Sharma, Water-stable metal-organic frameworks for aqueous removal of heavy metals and radionuclides: A review, *Chemosphere*, 2018, **209**, 783–800.
- 33 E. Doustkhah, R. Hassandoost, A. Khataee, R. Luque and M. H. N. Assadi, Hard-templated metal-organic frameworks for advanced applications, *Chem. Soc. Rev.*, 2021, **50**, 2927–2953.
- 34 Y. Yao, C. Wang, J. Na, M. S. A. Hossain, X. Yan, H. Zhang, M. A. Amin, J. Qi, Y. Yamauchi and J. Li, Macroscopic MOF architectures: Effective strategies for practical application in water treatment, *Small*, 2022, **18**, 2104387.
- 35 P. Cheng, C. Wang, Y. V. Kaneti, M. Eguchi, J. Lin, Y. Yamauchi and J. Na, Practical MOF nanoarchitectonics: New strategies for enhancing the processability of MOFs for practical applications, *Langmuir*, 2020, **36**, 4231–4249.
- 36 V. V. Butova, M. A. Soldatov, A. A. Guda, K. A. Lomachenko and C. Lamberti, Metal-organic frameworks: Structure, properties, methods of synthesis and characterization, *Russ. Chem. Rev.*, 2016, **85**, 280–307.
- 37 US Department of Health and Human Services, *Agency for Toxic Substances and Disease Registry-ATSDR*, 2018.
- 38 J. Li, X. Li, T. Hayat, A. Alsaedi and C. Chen, Screening of zirconium-based metal-organic frameworks for efficient simultaneous removal of antimonite (Sb(III)) and antimonate (Sb(V)) from aqueous solution, *ACS Sustainable Chem. Eng.*, 2017, **5**, 11496–11503.
- 39 W. Yu, M. Luo, Y. Yang, H. Wu, W. Huang, K. Zeng and F. Luo, Metal-organic framework (MOF) showing both ultrahigh As(V) and As(III) removal from aqueous solution, *J. Solid State Chem.*, 2019, **269**, 264–270.
- 40 C. Wang, X. Liu, J. P. Chen and K. Li, Superior removal of arsenic from water with zirconium metal-organic framework UiO-66, *Sci. Rep.*, 2015, **5**, 16613.
- 41 H. Atallah, M. Elcheikh Mahmoud, A. Jelle, A. Lough and M. Hmadeh, A highly stable indium based metal organic framework for efficient arsenic removal from water, *Dalton Trans.*, 2018, **47**, 799–806.
- 42 J. Cai, X. Wang, Y. Zhou, L. Jiang and C. Wang, Selective adsorption of arsenate and the reversible structure transformation of the mesoporous metal-organic framework MIL-100(Fe), *Phys. Chem. Chem. Phys.*, 2016, **18**, 10864–10867.
- 43 Y.-n. Wu, M. Zhou, B. Zhang, B. Wu, J. Li, J. Qiao, X. Guan and F. Li, Amino acid assisted templating synthesis of hierarchical zeolitic imidazolate framework-8 for efficient arsenate removal, *Nanoscale*, 2014, **6**, 1105–1112.
- 44 J. Sun, X. Zhang, A. Zhang and C. Liao, Preparation of Fe-Co based MOF-74 and its effective adsorption of arsenic from aqueous solution, *J. Environ. Sci.*, 2019, **80**, 197–207.
- 45 C. O. Audu, H. G. T. Nguyen, C.-Y. Chang, M. J. Katz, L. Mao, O. K. Farha, J. T. Hupp and S. T. Nguyen, The dual capture of As(V) and As(III) by UiO-66 and analogues, *Chem. Sci.*, 2016, **7**, 6492–6498.
- 46 C. Kang, Y. Peng, Y. Tang, H. Huang and C. Zhong, Sulfate-rich metal-organic framework for high efficiency and selective removal of barium from nuclear wastewater, *Ind. Eng. Chem. Res.*, 2017, **56**, 13866–13873.
- 47 Y. Peng, H. Huang, D. Liu and C. Zhong, Radioactive barium ion trap based on metal-organic framework for efficient and irreversible removal of barium from nuclear wastewater, *ACS Appl. Mater. Interfaces*, 2016, **8**, 8527–8535.
- 48 Y. Peng, H. Huang, Y. Zhang, C. Kang, S. Chen, L. Song, D. Liu and C. Zhong, A versatile MOF-based trap for heavy metal ion capture and dispersion, *Nat. Commun.*, 2018, **9**, 187.
- 49 H. Xue, Q. Chen, F. Jiang, D. Yuan, G. Lv, L. Liang, L. Liu and M. Hong, A regenerative metal-organic framework for reversible uptake of Cd(II): From effective adsorption to in situ detection, *Chem. Sci.*, 2016, **7**, 5983–5988.
- 50 K. Wang, J. Gu and N. Yin, Efficient removal of Pb(II) and Cd(II) Using NH<sub>2</sub>-functionalized Zr-MOFs via rapid microwave-promoted synthesis, *Ind. Eng. Chem. Res.*, 2017, **56**, 1880–1887.
- 51 Y. Wang, G. Ye, H. Chen, X. Hu, Z. Niu and S. Ma, Functionalized metal-organic framework as a new platform for efficient and selective removal of cadmium(II) from aqueous solution, *J. Mater. Chem. A*, 2015, **3**, 15292–15298.
- 52 H. Saleem, U. Rafique and R. P. Davies, Investigations on post-synthetically modified UiO-66-NH<sub>2</sub> for the adsorptive removal of heavy metal ions from aqueous solution, *Microporous Mesoporous Mater.*, 2016, **221**, 238–244.
- 53 E. Tahmasebi, M. Y. Masoomi, Y. Yamini and A. Morsali, Application of mechanothesized azine-decorated zinc(II) metal-organic frameworks for highly efficient removal and extraction of some heavy-metal ions from aqueous samples: A comparative study, *Inorg. Chem.*, 2015, **54**, 425–433.
- 54 H. Niu, Y. Zheng, S. Wang, S. He and Y. Cai, Stable hierarchical microspheres of 1D Fe-gallic acid MOFs for fast and efficient Cr(VI) elimination by a combination of reduction, metal substitution and coprecipitation, *J. Mater. Chem. A*, 2017, **5**, 16600–16604.
- 55 Q. Zhang, J. Yu, J. Cai, L. Zhang, Y. Cui, Y. Yang, B. Chen and G. Qian, A porous Zr-cluster-based cationic metal-organic framework for highly efficient Cr<sub>2</sub>O<sub>7</sub><sup>2-</sup> removal from water, *Chem. Commun.*, 2015, **51**, 14732–14734.
- 56 S.-Q. Deng, X.-J. Mo, S.-R. Zheng, X. Jin, Y. Gao, S.-L. Cai, J. Fan and W.-G. Zhang, Hydrolytically stable nanotubular cationic metal-organic framework for rapid and efficient removal of toxic oxo-anions and dyes from water, *Inorg. Chem.*, 2019, **58**, 2899–2909.
- 57 H.-R. Fu, Z.-X. Xu and J. Zhang, Water-stable metal-organic frameworks for fast and high dichromate trapping via single-crystal-to-single-crystal ion exchange, *Chem. Mater.*, 2015, **27**, 205–210.
- 58 H. Fei, C. S. Han, J. C. Robins and S. R. J. Oliver, A Cationic metal-organic solid solution based on Co(II) and Zn(II) for chromate trapping, *Chem. Mater.*, 2013, **25**, 647–652.
- 59 P.-F. Shi, B. Zhao, G. Xiong, Y.-L. Hou and P. Cheng, Fast capture and separation of, and luminescent probe for, pollutant chromate using a multi-functional cationic heterometal-organic framework, *Chem. Commun.*, 2012, **48**, 8231–8233.



- 60 H. Fei, M. R. Bresler and S. R. J. Oliver, A new Paradigm for Anion trapping in high capacity and selectivity: Crystal-to-crystal transformation of cationic materials, *J. Am. Chem. Soc.*, 2011, **133**, 11110–11113.
- 61 A. Maleki, B. Hayati, M. Naghizadeh and S. W. Joo, Adsorption of hexavalent chromium by metal organic frameworks from aqueous solution, *J. Ind. Eng. Chem.*, 2015, **28**, 211–216.
- 62 L.-L. Li, X.-Q. Feng, R.-P. Han, S.-Q. Zang and G. Yang, Cr(VI) removal via anion exchange on a silver-triazolate MOF, *J. Hazard. Mater.*, 2017, **321**, 622–628.
- 63 G. Yuan, Y. Tian, J. Liu, H. Tu, J. Liao, J. Yang, Y. Yang, D. Wang and N. Liu, Schiff base anchored on metal-organic framework for Co(II) removal from aqueous solution, *Chem. Eng. J.*, 2017, **326**, 691–699.
- 64 X. Luo, L. Ding and J. Luo, Adsorptive removal of Pb(II) ions from aqueous samples with amino-functionalization of metal-organic frameworks MIL-101(Cr), *J. Chem. Eng. Data*, 2015, **60**, 1732–1743.
- 65 L. Bai, B. Tu, Y. Qi, Q. Gao, D. Liu, Z. Liu, L. Zhao, Q. Li and Y. Zhao, Enhanced performance in gas adsorption and Li ion batteries by docking  $\text{Li}^+$  in a crown ether-based metal-organic framework, *Chem. Commun.*, 2016, **52**, 3003–3006.
- 66 M. Mon, F. Lloret, J. Ferrando-Soria, C. Martí-Gastaldo, D. Armentano and E. Pardo, Selective and efficient removal of mercury from aqueous media with the highly flexible arms of a BioMOF, *Angew. Chem., Int. Ed.*, 2016, **55**, 11167–11172.
- 67 Y. Wu, G. Xu, F. Wei, Q. Song, T. Tang, X. Wang and Q. Hu, Determination of Hg (II) in tea and mushroom samples based on metal-organic frameworks as solid phase extraction sorbents, *Microporous Mesoporous Mater.*, 2016, **235**, 204–210.
- 68 L. Liang, Q. Chen, F. Jiang, D. Yuan, J. Qian, G. Lv, H. Xue, L. Liu, H.-L. Jiang and M. Hong, In situ large-scale construction of sulfur-functionalized metal-organic framework and its efficient removal of Hg(II) from water, *J. Mater. Chem. A*, 2016, **4**, 15370–15374.
- 69 N. D. Rudd, H. Wang, E. M. A. Fuentes-Fernandez, S. J. Teat, F. Chen, G. Hall, Y. J. Chabal and J. Li, Highly efficient luminescent metal-organic framework for the simultaneous detection and removal of heavy metals from water, *ACS Appl. Mater. Interfaces*, 2016, **8**, 30294–30303.
- 70 Q.-R. Fang, D.-Q. Yuan, J. Sculley, J.-R. Li, Z.-B. Han and H.-C. Zhou, Functional mesoporous metal-organic frameworks for the capture of heavy metal ions and size-selective catalysis, *Inorg. Chem.*, 2010, **49**, 11637–11642.
- 71 K.-K. Yee, N. Reimer, J. Liu, S.-Y. Cheng, S.-M. Yiu, J. Weber, N. Stock and Z. Xu, Effective mercury sorption by thiol-laced metal-organic frameworks: In strong acid and the vapor phase, *J. Am. Chem. Soc.*, 2013, **135**, 7795–7798.
- 72 X. Luo, T. Shen, L. Ding, W. Zhong, J. Luo and S. Luo, Novel thymine-functionalized MIL-101 prepared by post-synthesis and enhanced removal of  $\text{Hg}^{2+}$  from water, *J. Hazard. Mater.*, 2016, **306**, 313–322.
- 73 S. Bhattacharjee, Y.-R. Lee and W.-S. Ahn, Post-synthesis functionalization of a zeolitic imidazolate structure ZIF-90: A study on removal of Hg(II) from water and epoxidation of alkenes, *CrystEngComm*, 2015, **17**, 2575–2582.
- 74 A. J. Howarth, M. J. Katz, T. C. Wang, A. E. Platero-Prats, K. W. Chapman, J. T. Hupp and O. K. Farha, High efficiency adsorption and removal of selenate and selenite from water using metal-organic frameworks, *J. Am. Chem. Soc.*, 2015, **137**, 7488–7494.
- 75 J. Wei, W. Zhang, W. Pan, C. Li and W. Sun, Experimental and theoretical investigations on Se(IV) and Se(VI) adsorption to UiO-66-based metal-organic frameworks, *Environ. Sci.: Nano*, 2018, **5**, 1441–1453.
- 76 J. Li, Y. Liu, X. Wang, G. Zhao, Y. Ai, B. Han, T. Wen, T. Hayat, A. Alsaedi and X. Wang, Experimental and theoretical study on selenate uptake to zirconium metal-organic frameworks: Effect of defects and ligands, *Chem. Eng. J.*, 2017, **330**, 1012–1021.
- 77 X. Cheng, M. Liu, A. Zhang, S. Hu, C. Song, G. Zhang and X. Guo, Size-controlled silver nanoparticles stabilized on thiol-functionalized MIL-53(Al) frameworks, *Nanoscale*, 2015, **7**, 9738–9745.
- 78 N. Zhang, L.-Y. Yuan, W.-L. Guo, S.-Z. Luo, Z.-F. Chai and W.-Q. Shi, Extending the use of highly porous and functionalized MOFs to Th(IV) capture, *ACS Appl. Mater. Interfaces*, 2017, **9**, 25216–25224.
- 79 X.-G. Guo, S. Qiu, X. Chen, Y. Gong and X. Sun, Postsynthesis modification of a metallosalen-containing metal-organic framework for selective Th(IV)/Ln(III) separation, *Inorg. Chem.*, 2017, **56**, 12357–12361.
- 80 Y. Feng, H. Jiang, S. Li, J. Wang, X. Jing, Y. Wang and M. Chen, Metal-organic frameworks HKUST-1 for liquid-phase adsorption of uranium, *Colloids Surf., A*, 2013, **431**, 87–92.
- 81 Z.-Q. Bai, L.-Y. Yuan, L. Zhu, Z.-R. Liu, S.-Q. Chu, L.-R. Zheng, J. Zhang, Z.-F. Chai and W.-Q. Shi, Introduction of amino groups into acid-resistant MOFs for enhanced U(VI) sorption, *J. Mater. Chem. A*, 2015, **3**, 525–534.
- 82 W. Yang, Z.-Q. Bai, W.-Q. Shi, L.-Y. Yuan, T. Tian, Z.-F. Chai, H. Wang and Z.-M. Sun, MOF-76: From a luminescent probe to highly efficient U(VI) sorption material, *Chem. Commun.*, 2013, **49**, 10415–10417.
- 83 M. Carboni, C. W. Abney, S. Liu and W. Lin, Highly porous and stable metal-organic frameworks for uranium extraction, *Chem. Sci.*, 2013, **4**, 2396–2402.
- 84 A. J. Howarth, A. W. Peters, N. A. Vermeulen, T. C. Wang, J. T. Hupp and O. K. Farha, Best practices for the synthesis, activation, and characterization of metal-organic frameworks, *Chem. Mater.*, 2017, **29**, 26–39.
- 85 K. S. Park, Z. Ni, A. P. Côté, J. Y. Choi, R. Huang, F. J. Uribe-Romo, H. K. Chae, M. O’Keeffe and O. M. Yaghi, Exceptional chemical and thermal stability of zeolitic imidazolate frameworks, *Proc. Natl. Acad. Sci. U. S. A.*, 2006, **103**, 10186.
- 86 A. J. Howarth, Y. Liu, P. Li, Z. Li, T. C. Wang, J. T. Hupp and O. K. Farha, Chemical, thermal and mechanical



- stabilities of metal–organic frameworks, *Nat. Rev. Mater.*, 2016, **1**, 15018.
- 87 N. M. Padial, E. Quartapelle Procopio, C. Montoro, E. López, J. E. Oltra, V. Colombo, A. Maspero, N. Masciocchi, S. Galli, I. Senkowska, S. Kaskel, E. Barea and J. A. R. Navarro, Highly hydrophobic isorecticular porous metal–organic frameworks for the capture of harmful volatile organic compounds, *Angew. Chem., Int. Ed.*, 2013, **52**, 8290–8294.
- 88 Q. Zha, X. Sang, D. Liu, D. Wang, G. Shi and C. Ni, Modification of hydrophilic amine-functionalized metal–organic frameworks to hydrophobic for dye adsorption, *J. Solid State Chem.*, 2019, **275**, 23–29.
- 89 S. Mukherjee, A. M. Kansara, D. Saha, R. Gonnade, D. Mullangi, B. Manna, A. V. Desai, S. H. Thorat, P. S. Singh, A. Mukherjee and S. K. Ghosh, An ultrahydrophobic fluorinated metal–organic framework derived recyclable composite as a promising platform to tackle marine oil spills, *Chem. – Eur. J.*, 2016, **22**, 10937–10943.
- 90 M. J. Katz, Z. J. Brown, Y. J. Colón, P. W. Siu, K. A. Scheidt, R. Q. Snurr, J. T. Hupp and O. K. Farha, A facile synthesis of UiO-66, UiO-67 and their derivatives, *Chem. Commun.*, 2013, **49**, 9449–9451.
- 91 J. B. DeCoste, G. W. Peterson, H. Jasuja, T. G. Glover, Y.-g. Huang and K. S. Walton, Stability and degradation mechanisms of metal–organic frameworks containing the  $Zr_6O_4(OH)_4$  secondary building unit, *J. Mater. Chem. A*, 2013, **1**, 5642–5650.
- 92 K. Leus, T. Bogaerts, J. De Decker, H. Depauw, K. Hendrickx, H. Vrielinck, V. Van Speybroeck and P. Van Der Voort, Systematic study of the chemical and hydrothermal stability of selected “stable” metal organic frameworks, *Microporous Mesoporous Mater.*, 2016, **226**, 110–116.
- 93 X. Liu, N. K. Demir, Z. Wu and K. Li, Highly water-stable zirconium metal–organic framework UiO-66 membranes supported on alumina hollow fibers for desalination, *J. Am. Chem. Soc.*, 2015, **137**, 6999–7002.
- 94 B. Wang, X.-L. Lv, D. Feng, L.-H. Xie, J. Zhang, M. Li, Y. Xie, J.-R. Li and H.-C. Zhou, Highly stable Zr(IV)-based metal–organic frameworks for the detection and removal of antibiotics and organic explosives in water, *J. Am. Chem. Soc.*, 2016, **138**, 6204–6216.
- 95 J. Yao, M. He, K. Wang, R. Chen, Z. Zhong and H. Wang, High-yield synthesis of zeolitic imidazolate frameworks from stoichiometric metal and ligand precursor aqueous solutions at room temperature, *CrystEngComm*, 2013, **15**, 3601–3606.
- 96 M. He, J. Yao, Q. Liu, K. Wang, F. Chen and H. Wang, Facile synthesis of zeolitic imidazolate framework-8 from a concentrated aqueous solution, *Microporous Mesoporous Mater.*, 2014, **184**, 55–60.
- 97 X.-L. Lv, S. Yuan, L.-H. Xie, H. F. Darke, Y. Chen, T. He, C. Dong, B. Wang, Y.-Z. Zhang, J.-R. Li and H.-C. Zhou, Ligand rigidification for enhancing the stability of metal–organic frameworks, *J. Am. Chem. Soc.*, 2019, **141**, 10283–10293.
- 98 S. Øien-Ødegaard, B. Bouchevreau, K. Hylland, L. Wu, R. Blom, C. Grande, U. Olsbye, M. Tilset and K. P. Lillerud, UiO-67-type metal–organic frameworks with enhanced water stability and methane adsorption capacity, *Inorg. Chem.*, 2016, **55**, 1986–1991.
- 99 J. Nagy, P. Bodart, I. Hannus and I. Kiricsi, *Characterization and Use of Zeolitic Microporous Materials*, DecaGen Ltd, 1998.
- 100 J. Gandara-Loe, L. Pastor-Perez, L. F. Bobadilla, J. A. Odriozola and T. R. Reina, Understanding the opportunities of metal–organic frameworks (MOFs) for CO<sub>2</sub> capture and gas-phase CO<sub>2</sub> conversion processes: A comprehensive overview, *React. Chem. Eng.*, 2021, **6**, 787–814.
- 101 B. Bueken, N. Van Velthoven, T. Willhammar, T. Stassin, I. Stassen, D. A. Keen, G. V. Baron, J. F. M. Denayer, R. Ameloot, S. Bals, D. De Vos and T. D. Bennett, Gel-based morphological design of zirconium metal–organic frameworks, *Chem. Sci.*, 2017, **8**, 3939–3948.
- 102 M. Kalaj, K. C. Bentz, S. Ayala, J. M. Palomba, K. S. Barcus, Y. Katayama and S. M. Cohen, MOF-polymer hybrid materials: From simple composites to tailored architectures, *Chem. Rev.*, 2020, **120**, 8267–8302.
- 103 B. Mohan, S. Kumar, Virender, A. Kumar, K. Kumar, K. Modi, T. Jiao and Q. Chen, Analogize of metal-organic frameworks (MOFs) adsorbents functional sites for Hg<sup>2+</sup> ions removal, *Sep. Purif. Technol.*, 2022, **297**, 121471.
- 104 J. Ouyang, J. Chen, S. Ma, X. Xing, L. Zhou, Z. Liu and C. Zhang, Adsorption removal of sulfamethoxazole from water using UiO-66 and UiO-66-BC composites, *Particuology*, 2022, **62**, 71–78.
- 105 Z. Inonu, S. Keskin and C. Erkey, An emerging family of hybrid nanomaterials: Metal–organic framework/aerogel composites, *ACS Appl. Nano Mater.*, 2018, **1**, 5959–5980.
- 106 H.-j. Qu, L.-j. Huang, Z.-y. Han, Y.-x. Wang, Z.-j. Zhang, Y. Wang, Q.-r. Chang, N. Wei, M. J. Kipper and J.-g. Tang, A review of graphene-oxide/metal–organic framework composites materials: Characteristics, preparation and applications, *J. Porous Mater.*, 2021, **28**, 1837–1865.
- 107 J. Darabdhara and M. Ahmaruzzaman, Recent developments in MOF and MOF based composite as potential adsorbents for removal of aqueous environmental contaminants, *Chemosphere*, 2022, **304**, 135261.
- 108 N. G. McCrum, C. Buckley, C. B. Bucknall and C. Bucknall, *Principles of polymer engineering*, Oxford University Press, 1997.
- 109 P. C. Painter and M. M. Coleman, *Fundamentals of polymer science: An introductory text*, Routledge, 2019.
- 110 D. Giliopoulos, A. Zamboulis, D. Giannakoudakis, D. Bikiaris and K. Triantafyllidis, Polymer/metal organic framework (MOF) nanocomposites for biomedical applications, *Molecules*, 2020, **25**, 185.
- 111 J. Chen, J. Ouyang, W. Chen, Z. Zheng, Z. Yang, Z. Liu and L. Zhou, Fabrication and adsorption mechanism of chitosan/Zr-MOF (UiO-66) composite foams for efficient removal of ketoprofen from aqueous solution, *Chem. Eng. J.*, 2022, **431**, 134045.
- 112 C. Wang, P. Cheng, Y. Yao, Y. Yamauchi, X. Yan, J. Li and J. Na, In-situ fabrication of nanoarchitected MOF filter for water purification, *J. Hazard. Mater.*, 2020, **392**, 122164.



- 113 T. Kitao, Y. Zhang, S. Kitagawa, B. Wang and T. Uemura, Hybridization of MOFs and polymers, *Chem. Soc. Rev.*, 2017, **46**, 3108–3133.
- 114 D. T. Sun, L. Peng, W. S. Reeder, S. M. Moosavi, D. Tiana, D. K. Britt, E. Oveisi and W. L. Queen, Rapid, selective heavy metal removal from water by a metal–organic framework/polydopamine composite, *ACS Cent. Sci.*, 2018, **4**, 349–356.
- 115 J. Li, Z. Wu, Q. Duan, A. Alsaedi, T. Hayat and C. Chen, Decoration of ZIF-8 on polypyrrole nanotubes for highly efficient and selective capture of U (VI), *J. Cleaner Prod.*, 2018, **204**, 896–905.
- 116 S. Yang, L. Peng, O. A. Syzgantseva, O. Trukhina, I. Kochetygov, A. Justin, D. T. Sun, H. Abedini, M. A. Syzgantseva, E. Oveisi, G. Lu and W. L. Queen, Preparation of highly porous metal–organic framework beads for metal extraction from liquid streams, *J. Am. Chem. Soc.*, 2020, **142**, 13415–13425.
- 117 J. Gascon and F. Kapteijn, Metal-organic framework membranes—high potential, bright future?, *Angew. Chem., Int. Ed.*, 2010, **49**, 1530–1532.
- 118 S.-z. Hu, T. Huang, N. Zhang, Y.-z. Lei and Y. Wang, Chitosan-assisted MOFs dispersion via covalent bonding interaction toward highly efficient removal of heavy metal ions from wastewater, *Carbohydr. Polym.*, 2022, **277**, 118809.
- 119 X.-X. Liang, N. Wang, Y.-L. Qu, L.-Y. Yang, Y.-G. Wang and X.-K. Ouyang, Facile preparation of metal-organic framework (MIL-125)/chitosan beads for adsorption of Pb (II) from aqueous solutions, *Molecules*, 2018, **23**, 1524.
- 120 K. Wang, X. Tao, J. Xu and N. Yin, Novel chitosan–MOF composite adsorbent for the removal of heavy metal ions, *Chem. Lett.*, 2016, **45**, 1365–1368.
- 121 J. E. Efome, D. Rana, T. Matsuura and C. Q. Lan, Insight studies on metal-organic framework nanofibrous membrane adsorption and activation for heavy metal ions removal from aqueous solution, *ACS Appl. Mater. Interfaces*, 2018, **10**, 18619–18629.
- 122 J. E. Efome, D. Rana, T. Matsuura and C. Q. Lan, Metal-organic frameworks supported on nanofibers to remove heavy metals, *J. Mater. Chem. A*, 2018, **6**, 4550–4555.
- 123 C. Lei, J. Gao, W. Ren, Y. Xie, S. Y. H. Abdalkarim, S. Wang, Q. Ni and J. Yao, Fabrication of metal-organic frameworks@cellulose aerogels composite materials for removal of heavy metal ions in water, *Carbohydr. Polym.*, 2019, **205**, 35–41.
- 124 S. Bo, W. Ren, C. Lei, Y. Xie, Y. Cai, S. Wang, J. Gao, Q. Ni and J. Yao, Flexible and porous cellulose aerogels/zeolitic imidazolate framework (ZIF-8) hybrids for adsorption removal of Cr (IV) from water, *J. Solid State Chem.*, 2018, **262**, 135–141.
- 125 H. Zhu, X. Yang, E. D. Cranston and S. Zhu, Flexible and porous nanocellulose aerogels with high loadings of metal–organic-framework particles for separations applications, *Adv. Mater.*, 2016, **28**, 7652–7657.
- 126 X. Ma, Y. Lou, X.-B. Chen, Z. Shi and Y. Xu, Multifunctional flexible composite aerogels constructed through in-situ growth of metal-organic framework nanoparticles on bacterial cellulose, *Chem. Eng. J.*, 2019, **356**, 227–235.
- 127 B. Han, E. Zhang and G. Cheng, Facile preparation of graphene oxide-MIL-101(Fe) composite for the efficient capture of uranium, *Appl. Sci.*, 2018, **8**, 2270.
- 128 P. Yang, Q. Liu, J. Liu, H. Zhang, Z. Li, R. Li, L. Liu and J. Wang, Correction: Interfacial growth of a metal–organic framework (UiO-66) on functionalized graphene oxide (GO) as a suitable seawater adsorbent for extraction of uranium(VI), *J. Mater. Chem. A*, 2018, **6**, 8121.
- 129 E. Rahimi and N. Mohaghegh, New hybrid nanocomposite of copper terephthalate MOF-graphene oxide: Synthesis, characterization and application as adsorbents for toxic metal ion removal from Sungun acid mine drainage, *Environ. Sci. Pollut. Res.*, 2017, **24**, 22353–22360.
- 130 K. Zhu, C. Chen, H. Xu, Y. Gao, X. Tan, A. Alsaedi and T. Hayat, Cr(VI) reduction and immobilization by core-double-shell structured magnetic polydopamine@zeolitic idazolate frameworks-8 microspheres, *ACS Sustainable Chem. Eng.*, 2017, **5**, 6795–6802.
- 131 Y. Xiong, F. Ye, C. Zhang, S. Shen, L. Su and S. Zhao, Synthesis of magnetic porous  $\gamma$ -Fe<sub>2</sub>O<sub>3</sub>/C@HKUST-1 composites for efficient removal of dyes and heavy metal ions from aqueous solution, *RSC Adv.*, 2015, **5**, 5164–5172.
- 132 R. Ricco, K. Konstas, M. J. Styles, J. J. Richardson, R. Babarao, K. Suzuki, P. Scopece and P. Falcaro, Lead (II) uptake by aluminium based magnetic framework composites (MFCs) in water, *J. Mater. Chem. A*, 2015, **3**, 19822–19831.
- 133 M. Taghizadeh, A. A. Asgharinezhad, M. Pooladi, M. Barzin, A. Abbaszadeh and A. Tadjarodi, A novel magnetic metal organic framework nanocomposite for extraction and preconcentration of heavy metal ions, and its optimization via experimental design methodology, *Microchim. Acta*, 2013, **180**, 1073–1084.
- 134 A. A. Alqadami, M. Naushad, Z. A. Allothman and A. A. Ghfar, Novel metal–organic framework (MOF) based composite material for the sequestration of U (VI) and Th (IV) metal ions from aqueous environment, *ACS Appl. Mater. Interfaces*, 2017, **9**, 36026–36037.
- 135 F. Ke, J. Jiang, Y. Li, J. Liang, X. Wan and S. Ko, Highly selective removal of Hg<sup>2+</sup> and Pb<sup>2+</sup> by thiol-functionalized Fe<sub>3</sub>O<sub>4</sub>@metal-organic framework core-shell magnetic microspheres, *Appl. Surf. Sci.*, 2017, **413**, 266–274.
- 136 J.-B. Huo, L. Xu, J.-C. E. Yang, H.-J. Cui, B. Yuan and M.-L. Fu, Magnetic responsive Fe<sub>3</sub>O<sub>4</sub>-ZIF-8 core-shell composites for efficient removal of As(III) from water, *Colloids Surf., A*, 2018, **539**, 59–68.
- 137 L. Huang, M. He, B. Chen and B. Hu, A designable magnetic MOF composite and facile coordination-based post-synthetic strategy for the enhanced removal of Hg<sup>2+</sup> from water, *J. Mater. Chem. A*, 2015, **3**, 11587–11595.
- 138 S. Naeimi and H. Faghihian, Modification and magnetization of MOF (HKUST-1) for the removal of Sr<sup>2+</sup> from aqueous solutions. Equilibrium, kinetic and thermodynamic modeling studies, *Sep. Sci. Technol.*, 2017, **52**, 2899–2908.



- 139 Z. Shi, C. Xu, H. Guan, L. Li, L. Fan, Y. Wang, L. Liu, Q. Meng and R. Zhang, Magnetic metal organic frameworks (MOFs) composite for removal of lead and malachite green in wastewater, *Colloids Surf., A*, 2018, **539**, 382–390.
- 140 M. Babazadeh, R. Hosseinzadeh-Khanmiri, J. Abolhasani, E. Ghorbani-Kalhor and A. Hassanpour, Solid phase extraction of heavy metal ions from agricultural samples with the aid of a novel functionalized magnetic metal-organic framework, *RSC Adv.*, 2015, **5**, 19884–19892.
- 141 N. Wang, X.-K. Ouyang, L.-Y. Yang and A. M. Omer, Fabrication of a magnetic cellulose nanocrystal/metal-organic framework composite for removal of Pb (II) from water, *ACS Sustainable Chem. Eng.*, 2017, **5**, 10447–10458.
- 142 S. E. Moradi, A. M. H. Shabani, S. Dadfarnia and S. Emami, Sulfonated metal organic framework loaded on iron oxide nanoparticles as a new sorbent for the magnetic solid phase extraction of cadmium from environmental water samples, *Anal. Methods*, 2016, **8**, 6337–6346.
- 143 W. Yang, Y. Qiang, M. Du, Y. Cao, Y. Wang, X. Zhang, T. Yue, J. Huang and Z. Li, Self-propelled nanomotors based on hierarchical metal-organic framework composites for the removal of heavy metal ions, *J. Hazard. Mater.*, 2022, **435**, 128967.
- 144 R. Ou, H. Zhang, V. X. Truong, L. Zhang, H. M. Hegab, L. Han, J. Hou, X. Zhang, A. Deletic, L. Jiang, G. P. Simon and H. Wang, A sunlight-responsive metal-organic framework system for sustainable water desalination, *Nat. Sustain.*, 2020, **12**, 1052–1058.
- 145 S. Zhang, R. Ou, H. Ma, J. Lu, M. M. Banaszak Holl and H. Wang, Thermally regenerable metal-organic framework with high monovalent metal ion selectivity, *Chem. Eng. J.*, 2020, **405**, 127037.
- 146 C. Ji, H. Yu, J. Lu, Y. Ren, L. Lv and W. Zhang, High-efficiency and sustainable desalination using thermo-regenerable MOF-808-EDTA: Temperature-regulated proton transfer, *ACS Appl. Mater. Interfaces*, 2021, **13**, 23833–23842.
- 147 H. Ma, Y. Yang, F. Yin, X.-F. Zhang, J. Qiu and J. Yao, Integration of thermoresponsive MIL-121 into alginate beads for efficient heavy metal ion removal, *J. Cleaner Prod.*, 2022, **333**, 130229.
- 148 F. Zou, R. Yu, R. Li and W. Li, Microwave-assisted synthesis of HKUST-1 and functionalized HKUST-1@H3PW12O40: Selective adsorption of heavy metal ions in water analyzed with synchrotron radiation, *ChemPhysChem*, 2013, **14**, 2825–2832.
- 149 J. Zhang, Z. Xiong, C. Li and C. Wu, Exploring a thiol-functionalized MOF for elimination of lead and cadmium from aqueous solution, *J. Mol. Liq.*, 2016, **221**, 43–50.
- 150 N. Yin, K. Wang and Z. Li, Novel melamine modified metal-organic frameworks for remarkably high removal of heavy metal Pb (II), *Desalination*, 2018, **430**, 120–127.
- 151 S. S. Kistler, Coherent expanded-aerogels, *J. Phys. Chem.*, 1932, **36**, 52–64.
- 152 Z. Ulker, I. Erucar, S. Keskin and C. Erkey, Novel nanostructured composites of silica aerogels with a metal organic framework, *Microporous Mesoporous Mater.*, 2013, **170**, 352–358.
- 153 P. Cheng, M. Kim, H. Lim, J. Lin, N. L. Torad, X. Zhang, M. S. A. Hossain, C.-W. Wu, C. Wang, J. Na and Y. Yamauchi, A general approach to shaped MOF-containing aerogels toward practical water treatment application, *Adv. Sustainable Syst.*, 2020, **4**, 2000060.
- 154 S. J. Yang, J. Y. Choi, H. K. Chae, J. H. Cho, K. S. Nahm and C. R. Park, Preparation and enhanced hydrostability and hydrogen storage capacity of CNT@MOF-5 hybrid composite, *Chem. Mater.*, 2009, **21**, 1893–1897.
- 155 S. Janakiram, J. L. Martín Espejo, X. Yu, L. Ansaloni and L. Deng, Facilitated transport membranes containing graphene oxide-based nanoplatelets for CO<sub>2</sub> separation: Effect of 2D filler properties, *J. Membr. Sci.*, 2020, **616**, 118626.
- 156 W. Wei, Z. Liu, R. Wei, G.-C. Han and C. Liang, Synthesis of MOFs/GO composite for corrosion resistance application on carbon steel, *RSC Adv.*, 2020, **10**, 29923–29934.
- 157 T. J. Bandosz and C. Petit, MOF/graphite oxide hybrid materials: Exploring the new concept of adsorbents and catalysts, *Adsorption*, 2011, **17**, 5–16.
- 158 S. Singamaneni, V. N. Bliznyuk, C. Binek and E. Y. Tsymbal, Magnetic nanoparticles: Recent advances in synthesis, self-assembly and applications, *J. Mater. Chem.*, 2011, **21**, 16819–16845.
- 159 L. Melag, M. M. Sadiq, K. Konstas, F. Zadehahmadi, K. Suzuki and M. R. Hill, Performance evaluation of CuBTC composites for room temperature oxygen storage, *RSC Adv.*, 2020, **10**, 40960–40968.
- 160 H. Li, M. M. Sadiq, K. Suzuki, P. Falcaro, A. J. Hill and M. R. Hill, Magnetic induction framework synthesis: A general route to the controlled growth of metal-organic frameworks, *Chem. Mater.*, 2017, **29**, 6186–6190.
- 161 R. Xiao, Y. Pan, J. Li, L. Zhang and W. Zhang, Layer-by-layer assembled magnetic bimetallic metal-organic framework composite for global phosphopeptide enrichment, *J. Chromatogr. A*, 2019, **1601**, 45–52.
- 162 B. E. Meteku, J. Huang, J. Zeng, F. Subhan, F. Feng, Y. Zhang, Z. Qiu, S. Aslam, G. Li and Z. Yan, Magnetic metal-organic framework composites for environmental monitoring and remediation, *Coord. Chem. Rev.*, 2020, **413**, 213261.
- 163 A. Sharma, D. Mangla, Shehnaz and S. A. Chaudhry, Recent advances in magnetic composites as adsorbents for wastewater remediation, *J. Environ. Manage.*, 2022, **306**, 114483.
- 164 R. Ma, P. Yang, Y. Ma and F. Bian, Facile synthesis of magnetic hierarchical core-shell structured Fe<sub>3</sub>O<sub>4</sub>@PDA-Pd@MOF nanocomposites: Highly integrated multifunctional catalysts, *ChemCatChem*, 2018, **10**, 1446–1454.
- 165 K. Li, S. Zou, G. Jin, J. Yang, M. Dou, L. Qin, H. Su and F. Huang, Efficient removal of selenite in aqueous solution by MOF-801 and Fe<sub>3</sub>O<sub>4</sub>/MOF-801: Adsorptive behavior and mechanism study, *Sep. Purif. Technol.*, 2022, **296**, 121384.
- 166 M. Iranmanesh and J. Hulliger, Magnetic separation: its application in mining, waste purification, medicine,





- biochemistry and chemistry, *Chem. Soc. Rev.*, 2017, **46**, 5925–5934.
- 167 S. Yadav, R. Dixit, S. Sharma, S. Dutta, K. Solanki and R. K. Sharma, Magnetic metal–organic framework composites: Structurally advanced catalytic materials for organic transformations, *Mater. Adv.*, 2021, **2**, 2153–2187.
- 168 W. A. El-Mehalmey, A. H. Ibrahim, A. A. Abugable, M. H. Hassan, R. R. Haikal, S. G. Karakalos, O. Zaki and M. H. Alkordi, Metal–organic framework@silica as a stationary phase sorbent for rapid and cost-effective removal of hexavalent chromium, *J. Mater. Chem. A*, 2018, **6**, 2742–2751.
- 169 G. Crini, E. Lichtfouse, L. D. Wilson and N. Morin-Crini, Conventional and non-conventional adsorbents for wastewater treatment, *Environ. Chem. Lett.*, 2019, **17**, 195–213.
- 170 Y. Jiang, P. Tan, X.-Q. Liu and L.-B. Sun, Process-oriented smart adsorbents: Tailoring the properties dynamically as demanded by adsorption/desorption, *Acc. Chem. Res.*, 2022, **55**, 75–86.
- 171 A. Ihsanullah, A. Abbas, M. Al-Amer, T. Laoui, M. J. Al-Marri, M. S. Nasser, M. Khraisheh and M. A. Atieh, Heavy metal removal from aqueous solution by advanced carbon nanotubes: Critical review of adsorption applications, *Sep. Purif. Technol.*, 2016, **157**, 141–161.
- 172 N. A. Khan, Z. Hasan and S. H. Jhung, Adsorptive removal of hazardous materials using metal-organic frameworks (MOFs): A review, *J. Hazard. Mater.*, 2013, **244–245**, 444–456.
- 173 H. S. Cho, H. Tanaka, Y. Lee, Y.-B. Zhang, J. Jiang, M. Kim, H. Kim, J. K. Kang and O. Terasaki, Physicochemical understanding of the impact of pore environment and species of adsorbates on adsorption behaviour, *Angew. Chem., Int. Ed.*, 2021, **60**, 20504–20510.
- 174 B. Mohan, A. Kamboj, Virender, K. Singh, Priyanka, G. Singh, A. J. L. Pombeiro and P. Ren, Metal-organic frameworks (MOFs) materials for pesticides, heavy metals, and drugs removal: Environmental safety, *Sep. Purif. Technol.*, 2023, **310**, 123175.
- 175 I. Ahmed, Z. Hasan, G. Lee, H. J. Lee and S. H. Jhung, Contribution of hydrogen bonding to liquid-phase adsorptive removal of hazardous organics with metal-organic framework-based materials, *Chem. Eng. J.*, 2022, **430**, 132596.
- 176 I. Ahmed and S. H. Jhung, Adsorptive desulfurization and denitrogenation using metal-organic frameworks, *J. Hazard. Mater.*, 2016, **301**, 259–276.
- 177 Z.-M. Liu, S.-H. Wu, S.-Y. Jia, F.-X. Qin, S.-M. Zhou, H.-T. Ren, P. Na and Y. Liu, Novel hematite nanorods and magnetite nanoparticles prepared from MIL-100(Fe) template for the removal of As(V), *Mater. Lett.*, 2014, **132**, 8–10.
- 178 Z. Hasan and S. H. Jhung, Removal of hazardous organics from water using metal-organic frameworks (MOFs): Plausible mechanisms for selective adsorptions, *J. Hazard. Mater.*, 2015, **283**, 329–339.
- 179 E. Herrero, J. M. Feliu, S. Blais, Z. Radovic-Hrapovic and G. Jerkiewicz, Temperature dependence of CO chemisorption and its oxidative desorption on the Pt(111) electrode, *Langmuir*, 2000, **16**, 4779–4783.
- 180 A. Abbasi, T. Moradpour and K. Van Hecke, A new 3D cobalt (II) metal–organic framework nanostructure for heavy metal adsorption, *Inorg. Chim. Acta*, 2015, **430**, 261–267.
- 181 A. Heidari, H. Younesi, A. Rashidi and A. Ghoreyshi, Adsorptive removal of CO<sub>2</sub> on highly microporous activated carbons prepared from Eucalyptus camaldulensis wood: Effect of chemical activation, *J. Taiwan Inst. Chem. Eng.*, 2014, **45**, 579–588.
- 182 L. Esrafil, M. Gharib and A. Morsali, The targeted design of dual-functional metal–organic frameworks (DF-MOFs) as highly efficient adsorbents for Hg<sup>2+</sup> ions: Synthesis for purpose, *Dalton Trans.*, 2019, **48**, 17831–17839.
- 183 H. Xue, Q. Chen, F. Jiang, D. Yuan, G. Lv, L. Liang, L. Liu and M. Hong, A regenerative metal–organic framework for reversible uptake of Cd(II): From effective adsorption to in situ detection, *Chem. Sci.*, 2016, **7**, 5983–5988.
- 184 Y. Chen, X. Bai and Z. Ye, Recent progress in heavy metal ion decontamination based on metal–organic frameworks, *Nanomaterials*, 2020, **10**, 1481.
- 185 N. Manousi, D. A. Giannakoudakis, E. Rosenberg and G. A. Zachariadis, Extraction of metal ions with metal–organic frameworks, *Molecules*, 2019, **24**, 4605.
- 186 B. Liu, M. Jian, R. Liu, J. Yao and X. Zhang, Highly efficient removal of arsenic(III) from aqueous solution by zeolitic imidazolate frameworks with different morphology, *Colloids Surf., A*, 2015, **481**, 358–366.
- 187 C. W. Abney, J. C. Gilhula, K. Lu and W. Lin, Metal-organic framework templated inorganic sorbents for rapid and efficient extraction of heavy metals, *Adv. Mater.*, 2014, **26**, 7993–7997.
- 188 M. Moradi, Mercuric chloride adsorption on sulfur-containing BC<sub>2</sub>N nanotube: Toward HSAB concept, *Struct. Chem.*, 2014, **25**, 1091–1097.
- 189 J. Kammerer, R. Carle and D. R. Kammerer, Adsorption and ion exchange: Basic principles and their application in food processing, *J. Agric. Food Chem.*, 2011, **59**, 22–42.
- 190 S. S. Ray, R. Gusain and N. Kumar, *Carbon nanomaterial-based adsorbents for water purification: Fundamentals and applications*, Elsevier, 2020, pp. 67–100.
- 191 L. Aboutorabi, A. Morsali, E. Tahmasebi and O. Büyükgüngör, Metal–organic framework based on isonicotinate n-oxide for fast and highly efficient aqueous phase Cr(VI) adsorption, *Inorg. Chem.*, 2016, **55**, 5507–5513.
- 192 X. Li, X. Gao, L. Ai and J. Jiang, Mechanistic insight into the interaction and adsorption of Cr(VI) with zeolitic imidazolate framework-67 microcrystals from aqueous solution, *Chem. Eng. J.*, 2015, **274**, 238–246.
- 193 S. Rapti, A. Pournara, D. Sarma, I. T. Papadas, G. S. Armatas, Y. S. Hassan, M. H. Alkordi, M. G. Kanatzidis and M. J. Manos, Rapid, green and inexpensive synthesis



- of high quality UiO-66 amino-functionalized materials with exceptional capability for removal of hexavalent chromium from industrial waste, *Inorg. Chem. Front.*, 2016, **3**, 635–644.
- 194 Z.-H. Zhang, J.-H. Lan, L.-Y. Yuan, P.-P. Sheng, M.-Y. He, L.-R. Zheng, Q. Chen, Z.-F. Chai, J. K. Gibson and W.-Q. Shi, Rational construction of porous metal–organic frameworks for uranium(VI) extraction: The strong periodic tendency with a metal node, *ACS Appl. Mater. Interfaces*, 2020, **12**, 14087–14094.
- 195 T. A. Vu, G. H. Le, C. D. Dao, L. Q. Dang, K. T. Nguyen, Q. K. Nguyen, P. T. Dang, H. T. Tran, Q. T. Duong and T. V. Nguyen, Arsenic removal from aqueous solutions by adsorption using novel MIL-53 (Fe) as a highly efficient adsorbent, *RSC Adv.*, 2015, **5**, 5261–5268.
- 196 N. C. Burtch, H. Jasuja and K. S. Walton, Water stability and adsorption in metal–organic frameworks, *Chem. Rev.*, 2014, **114**, 10575–10612.
- 197 J. Canivet, A. Fateeva, Y. Guo, B. Coasne and D. Farrusseng, Water adsorption in MOFs: Fundamentals and applications, *Chem. Soc. Rev.*, 2014, **43**, 5594–5617.
- 198 K. Tan, N. Nijem, Y. Gao, S. Zuluaga, J. Li, T. Thonhauser and Y. J. Chabal, Water interactions in metal organic frameworks, *CrystEngComm*, 2015, **17**, 247–260.
- 199 P. Kumar, B. Anand, Y. F. Tsang, K.-H. Kim, S. Khullar and B. Wang, Regeneration, degradation, and toxicity effect of MOFs: Opportunities and challenges, *Environ. Res.*, 2019, **176**, 108488.
- 200 C. Wang, X. Liu, N. Keser Demir, J. P. Chen and K. Li, Applications of water stable metal–organic frameworks, *Chem. Soc. Rev.*, 2016, **45**, 5107–5134.
- 201 C.-X. Chen, Y.-Z. Fan, C.-C. Cao, H.-P. Wang, Y.-N. Fan, J.-J. Jiang, Z.-W. Wei, G. Maurin and C.-Y. Su, Dynamic coordination chemistry of fluorinated Zr-MOFs: Synthetic control and reassembly/disassembly beyond de novo synthesis to tune the structure and property, *Chem. – Eur. J.*, 2020, **26**, 8254–8261.
- 202 V. V. Butova, I. A. Pankin, O. A. Burachevskaya, K. S. Vetlitsyna-Novikova and A. V. Soldatov, New fast synthesis of MOF-801 for water and hydrogen storage: Modulator effect and recycling options, *Inorg. Chim. Acta*, 2021, **514**, 120025.

